AD-A060 433 TEXAS UNIV AT EL PASO DEPT OF ELECTRICAL ENGINEERING F/G 4/1
A SUBSONIC GERDIEN CONDENSER EXPERIMENT FOR UPPER ATMOSPHERIC R--ETC(U)
AUG 78 R S SAGAR, J D MITCHELL DAAD07-74-C-0263
UNCLASSIFIED ERADCOM/ASL-CR-78-0263-3 NL

1 OF 1
AD A060 433

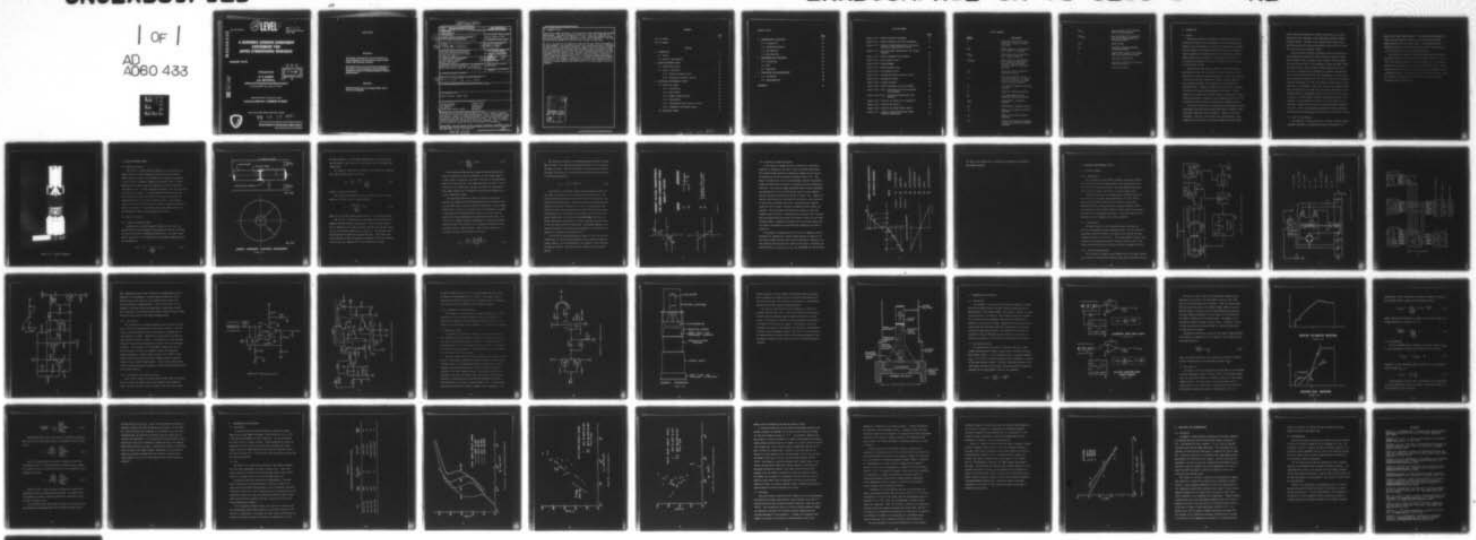

END
DATE FILMED
1-79
DDC

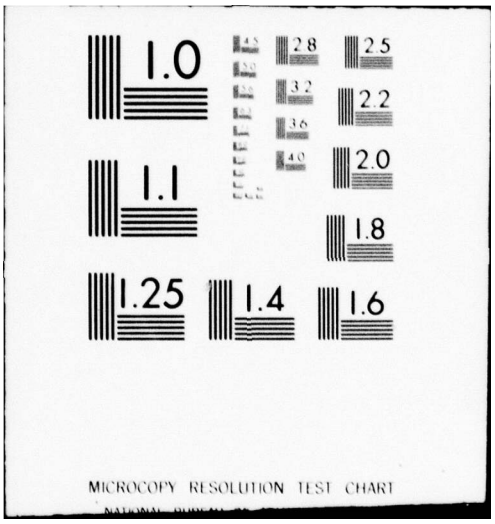
1.0
1.1
1.25
1.4
1.6
1.8
2.0
2.2
2.5
2.8
3.2
3.6
4.0
MICROCOPY RESOLUTION TEST CHART

(12) LEVEL II

ASL-CR-78-0263-3

AD

Reports Control Symbol
OSD - 1366

AD A060433

A SUBSONIC GERDIEN CONDENSER EXPERIMENT FOR UPPER ATMOSPHERIC RESEARCH

AUGUST 1978

Prepared by

R. S. SAGAR

J.D. MITCHELL

Electrical Engineering Department

THE UNIVERSITY OF TEXAS at EL PASO

UNDER CONTRACT DAAD07-74-C-0263

Contract Monitor: ROBERT OLSEN

US Army Electronics Research and Development Command

Atmospheric Sciences Laboratory

White Sands Missile Range, NM 88002

NOTICES

Disclaimers

The findings in this report are not to be construed as an official Department of the Army position, unless so designated by other authorized documents.

The citation of trade names and names of manufacturers in this report is not to be construed as official Government indorsement or approval of commercial products or services referenced herein.

Disposition

Destroy this report when it is no longer needed. Do not return it to the originator.

(18) ERADCOM/ASL

SECURITY CLASSIFICATION OF THIS PAGE (When Data Entered)

(19) **REPORT DOCUMENTATION PAGE**

READ INSTRUCTIONS BEFORE COMPLETING FORM

1. REPORT NUMBER: ASL-CR-78-0263-3 ✓
2. GOVT ACCESSION NO.
3. RECIPIENT'S CATALOG NUMBER

(6) 4. TITLE (and Subtitle): A SUBSONIC GERDIEN CONDENSER EXPERIMENT FOR UPPER ATMOSPHERIC RESEARCH,

5. TYPE OF REPORT & PERIOD COVERED: Special Report 6-16-78

6. PERFORMING ORG. REPORT NUMBER

(10) 7. AUTHOR(s): R. S. Sagar and J. D. Mitchell

(15) 8. CONTRACT OR GRANT NUMBER(s): DAAD07-74-C-0263 ✓

9. PERFORMING ORGANIZATION NAME AND ADDRESS
Electrical Engineering Department ✓
The University of Texas at El Paso
El Paso, TX 79968

10. PROGRAM ELEMENT, PROJECT, TASK AREA & WORK UNIT NUMBERS
DA Task 1L161102B53A, SA2
(16)

11. CONTROLLING OFFICE NAME AND ADDRESS
US Army Electronics Research and Development Command
Adelphi, MD 20783
(11)

12. REPORT DATE: August 1978 (17)

13. NUMBER OF PAGES: 51

14. MONITORING AGENCY NAME & ADDRESS (if different from Controlling Office)
Atmospheric Sciences Laboratory
White Sands Missile Range, NM 88002
(12) 55p.

15. SECURITY CLASS. (of this report): UNCLASSIFIED

15a. DECLASSIFICATION/DOWNGRADING SCHEDULE

16. DISTRIBUTION STATEMENT (of this Report)

Approved for public release; distribution unlimited.

(9) Special rept. for period ending 16 Jun 78,

17. DISTRIBUTION STATEMENT (of the abstract entered in Block 20, if different from Report)

18. SUPPLEMENTARY NOTES

Contract monitor: Robert Olsen

19. KEY WORDS (Continue on reverse side if necessary and identify by block number)

Gerdien condenser	Positive ions
Ion conductivity	Negative ions
Ion mobility	Stratosphere
Rocket-borne subsonic sensor	Mesosphere

20. ABSTRACT (Continue on reverse side if necessary and identify by block number)

This research is concerned with the design of a Gerdien condenser experiment suitable for flight on a standard meteorological rocket. After separating from the rocket at apogee, the instrument descends on a stabilized parachute system, telemetering the data back to ground while in flight. The theory of charged particle collection is presented for the Gerdien condenser. Also, the electrical and mechanical design for the particular system is discussed.

Measurements from two subsonic Gerdien condenser experiments conducted at White

DD FORM 1 JAN 73 1473 EDITION OF 1 NOV 65 IS OBSOLETE

LB

SECURITY CLASSIFICATION OF THIS PAGE (When Data Entered)

408 579

20. ABSTRACT (cont)

Sands Missile Range, New Mexico, during morning twilight conditions are presented and analyzed. The same instrument was flown on 15 July 1975 at 0618 MST (χ = 75°) and 26 September 1975 at 0600 MST (χ = 90°). Electrical conductivity data from two subsonic blunt probe experiments [9 June 1971 at 0809 MST (χ = 53°) and 28 July 1971 at 0705 MST (χ = 68°)] are also included in this study.

At 30 km, the positive ion conductivity data for the four flights are generally in good agreement, thus indicating no particular discrepancies due to differences in launch dates or measurement techniques. Above 60 km, the buildup in conductivity with respect to the launch times presumably reflects an increase in positive ion number density associated with solar ultraviolet ionization. The most noticeable buildup, however, occurs between 35 and 60 km where the positive ion conductivity values increase during the early morning period by as much as an order of magnitude (between 45 and 50 km). The Gerdien condenser measurements indicate that this buildup in conductivity is related to an increase in positive ion mobility, thus suggesting the presence during the early morning hours of a process for forming smaller, more mobile positive ions which appear to be solar dependent.

CONTENTS

	Page
LIST OF FIGURES	3
LIST OF SYMBOLS	4

CHAPTERS

1. INTRODUCTION	6
1.1 Review	6
1.2 Scope of this Research	7
2. GERDIEN CONDENSER THEORY	10
2.1 General Description	10
2.2 Theory of Operation	10
2.2.1 Single Ion Mobility Case	10
2.2.2 Multiple Ion Mobility Species	16
3. ELECTRICAL AND MECHANICAL DESIGN	19
3.1 Electrical Design	19
3.1.1 Introduction	19
3.1.2 Power Supply	19
3.1.3 Sweep Voltage Generator	19
3.1.4 Electrometer	24
3.1.5 Voltage-Pulse Rate Converter Circuit	24
3.1.6 Transmitter and Antenna System	27
3.2 Mechanical Design	27

Contents (cont)

	Page
4. TELEMETRY/DATA ACQUISITION	32
4.1 Introduction	32
4.2 Calibration Waveform	32
4.3 Data Waveform	34
4.4 Data Reduction	36
5. MEASUREMENTS AND DISCUSSION	39
5.1 Introduction	39
5.2 Data	39
5.3 Discussion	44
6. CONCLUSIONS AND RECOMMENDATIONS	48
6.1 Conclusions	48
6.2 Recommendations	49
REFERENCES	50

LIST OF FIGURES

	Page
Figure (1-1) - Gerdien Condenser Photograph	9
Figure (2-1) - Gerdien Condenser Electrode Arrangement	11
Figure (2-2) - Current-Voltage Characteristic for Gerdien Condenser--Single Mobility Species	15
Figure (2-3) - Current-Voltage Characteristic for Gerdien Condenser	17
Figure (3-1) - Gerdien Condenser Block Diagram	20
Figure (3-2) - Power Supply Circuit	21
Figure (3-3) - Wiring Diagram	22
Figure (3-4) - Sweep Voltage Circuit	23
Figure (3-5) - Electrometer Circuit	25
Figure (3-6) - Voltage-Pulse Rate Converter Circuit	26
Figure (3-7) - Transmitter Circuit	28
Figure (3-8) - Gerdien Condenser	29
Figure (3-9) - Gerdien Condenser Collector Assembly	31
Figure (4-1a, 4-1b) - Calibration and Operating Modes Block Diagram	33
Figure (4-2a, 4-2b) - Calibration Waveform and Data Waveform	35
Figure (5-1) - Positive Ion Conductivity (Composite)	41
Figure (5-2) - Positive Ion Mobility	42
Figure (5-3) - Positive Ion Charge Number Density	43
Figure (5-4) - Secant of Solar Zenith Angle Versus Positive Conductivity	47

LIST OF SYMBOLS

Symbol	Definitions
C	Capacitance between the inner (collector) and outer (return) electrodes
$E(r)$	Radial component of the electric field inside the condenser
$(i)_{cal}$	Input current to the electrometer during calibration
$(i_{\pm})_{Data}$	Input current to the electrometer during the flight/data portion of the instrument's operation (subscript indicates polarity)
$i_{s\pm}$	Saturation current (subscript indicates polarity)
$i_{\pm}$	Collection current, used to describe current due to charged particle collection only (subscript indicates polarity)
$k_{\pm}$	Ion mobility (subscript indicates polarity)
ℓ	Length of collector electrode
$N_{\pm}$	Ion charge number density (subscript indicates polarity)
R_{cal}	Electrometer's calibration resistor
R_f	Electrometer's feedback resistor
r_i	Radius of the inner (collector) electrode
r_o	Radius of the outer (return) electrode
$\langle v \rangle$	Average flow velocity associated with an ion entering the Gerdien condenser

$(V)_{cal}$	Output voltage of the electrometer during calibration
$(V_{\pm})_{Data}$	Output voltage of the electrometer during flight (subscript indicates polarity)
$V(t)$	Sweep voltage
$V_{s\pm}$	Saturation voltage (subscript indicates polarity)
v_r	Radial drift velocity for charged particles inside the aspirator
ε	Free space permittivity
$\sigma_{\pm}$	Electrical conductivity (subscript indicates polarity)
χ	Solar zenith angle

1. INTRODUCTION

1.1 Review

The current interest in atmospheric research with respect to ionization processes in the stratosphere and lower mesosphere has resulted in the development of specialized instrumentation systems. One such system is the Gerdien condenser which uses a cylindrical collector geometry for measuring electrical conductivity, charge number density and ion mobility. The instrument is named for H. Gerdien who presented the theory of charge particle collection for this device in 1905.

Early work with the Gerdien condenser included ion mobility experiments at sea level as reported by Israel and Schulz (1933). Balloon borne Gerdien condenser experiments for measuring electrical conductivity have been conducted by Stergis, Coroniti, Nazarek, Kota, Seymour and Werme (1955), Woessner and Cobb (1958) and Paltridge (1965). Kraakevik (1958) utilized the Gerdien condenser for electrical conductivity measurements on aircraft. In this research, the accumulation of static charge on wing surfaces during flight necessitated an analysis of the resulting electric field and the effect it might have on the collection of charged particles.

Electrical conductivity, ion mobility and charge number density measurements have also been obtained from Gerdien condenser rocket experiments employing either supersonic or subsonic collection techniques. Electrical conductivity data from supersonic rocket flights have been reported by Bourdeau, Whipple and Clark (1959).

Conley (1974) has published ion mobility and positive ion concentration data from supersonic rocket experiments using the Gerdien condenser system. Included in this research was a study of how the collected positive ions would possibly be affected by the shock wave associated with supersonic flight.

Subsonic Gerdien condenser experiments flown on parachute systems deployed from rockets have been conducted by Pederson (1964), Rose and Widdel (1972), Farrokh (1975), Croskey (1976) and Widdel, Rose and Borchers (1976). The experiments of Rose and Widdel (1972) and Widdel et al. (1976) utilized a Gerdien condenser with an air flow meter accompanying the instrument in a parallel configuration. The air flow data obtained from their experiments in the laboratory and on parachutes indicated that the ion flow velocity for a Gerdien condenser descending on a stabilized parachute system could be estimated from the instrument's radar fall velocity data [Widdel (1975)]. Thus, the ability to use these radar data greatly simplifies the instrument design by eliminating the need for such an air flow measuring device. For the Gerdien condenser experiments reported in this research, a cross parachute was used on the first flight (July 15, 1975) and a starute was flown with the second experiment (September 26, 1975). Both of these parachute systems have been developed to minimize payload swing typically associated with decelerator systems.

1.2 Scope of this Research

The objective of this research was to design a subsonic Gerdien condenser experiment for measuring electrical conductivity, ion

mobility and charge number density. The instrument was designed for flight on rocket systems currently in use by the Meteorological Rocket Network such as the Arcas rocket. As discussed earlier, a stabilized parachute system was used since the ion flow velocity was to be calculated from the instrument's radar data.

The two Gerdien condenser experiments reported in this research were both conducted at White Sands Missile Range, New Mexico. A picture of the Gerdien condenser is shown in Figure (1-1). The instrument was first launched on July 15, 1975 at 0618 MST (χ=75°). After being successfully recovered, it was flown again on September 26, 1975 at 0600 MST (χ=90°). The launch times were selected in order to study the ionization variability in the midlatitude, middle atmosphere during the early morning period.

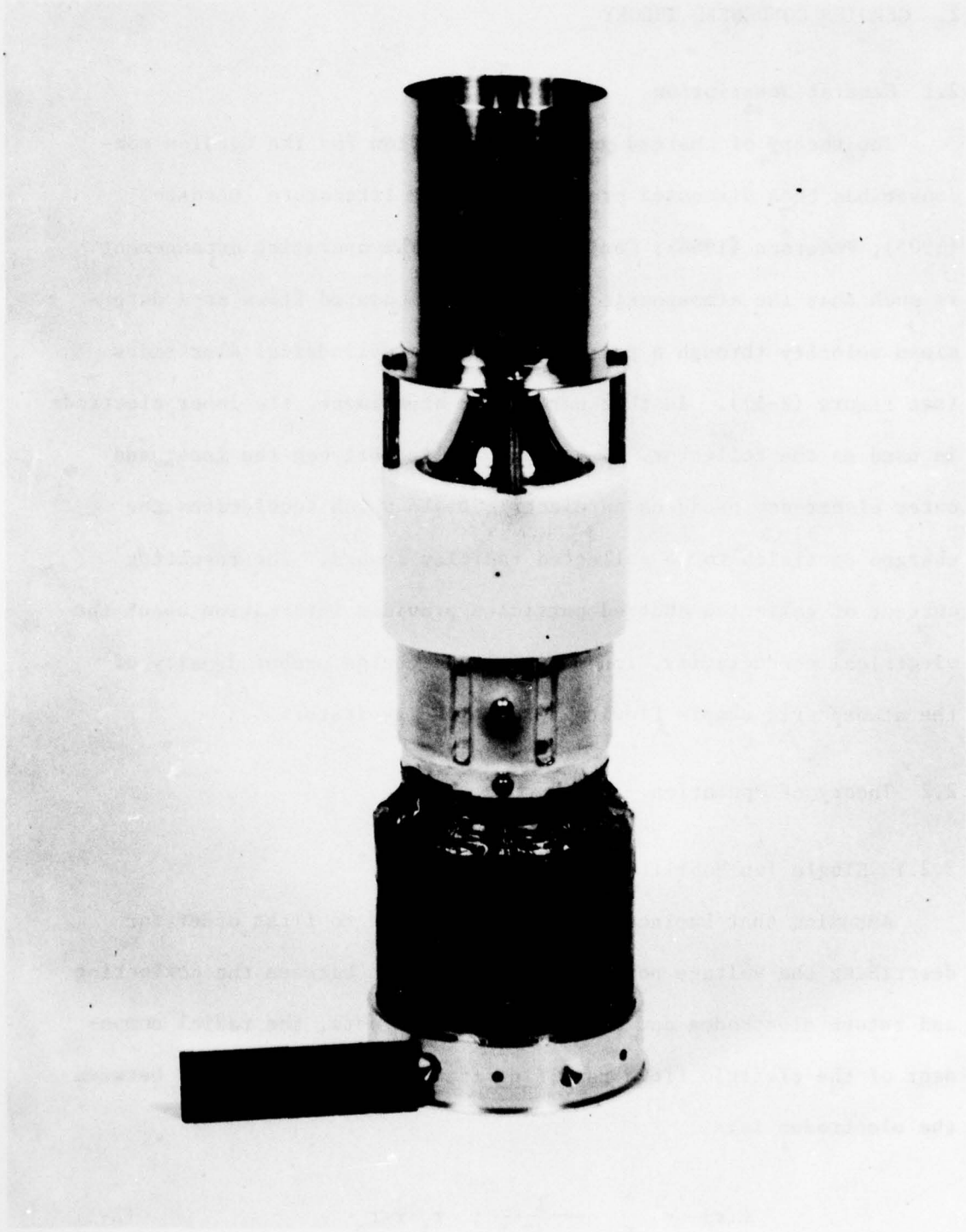

Figure (1-1) - Gerdien Condenser

2. GERDIEN CONDENSER THEORY

2.1 General Description

The theory of charged particle collection for the Gerdien condenser has been discussed previously in the literature [Gerdien (1905); Pederson (1964); Conley (1974)]. The operating arrangement is such that the atmospheric sample to be measured flows at a determined velocity through a pair of concentric cylindrical electrodes (see Figure (2-1)). In this particular experiment, the inner electrode is used as the collector. A voltage applied between the inner and outer electrodes produces an electric field which accelerates the charged particles to be collected radially inward. The resulting current of collected charged particles provides information about the electrical conductivity, ion mobility and charge number density of the atmospheric sample flowing through the aspirator.

2.2 Theory of Operation

2.2.1 Single Ion Mobility Case

Assuming that Laplace's equation is valid to first order for describing the voltage potential in the region between the collecting and return electrodes and neglecting edge effects, the radial component of the electric field resulting from a voltage V applied between the electrodes is:

$$E(r) = \frac{V}{r} \frac{1}{\ln\left(\frac{r_o}{r_i}\right)} ; \quad r_i < r < r_o \qquad (2\text{-}1)$$

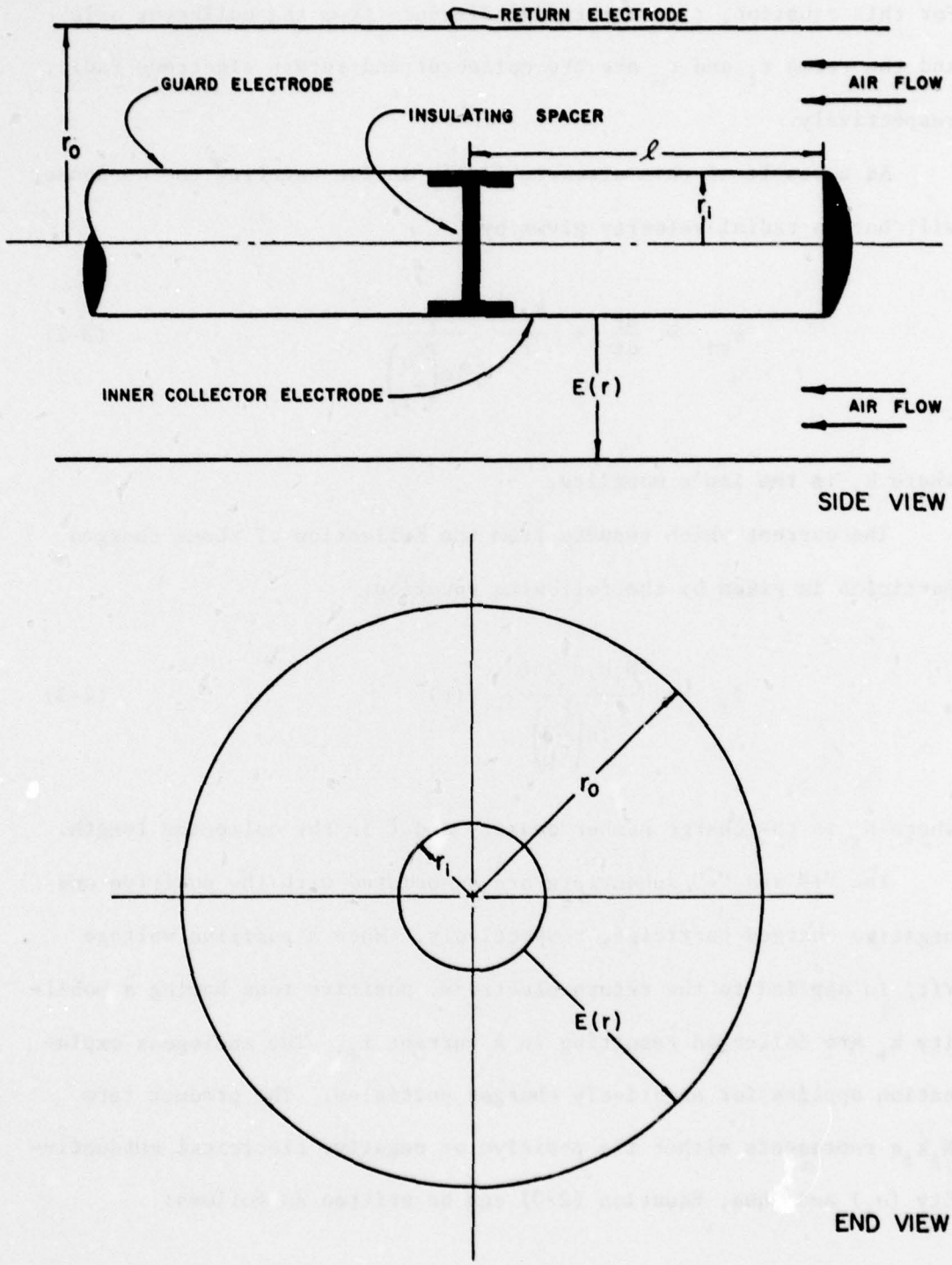

GERDIEN CONDENSER ELECTRODE ARRANGEMENT

FIGURE (2-1)

For this equation, r is the radial distance from the collector axis and the terms r_i and r_o are the collector and return electrode radii, respectively.

As a result of this electric field, an ion entering the condenser will have a radial velocity given by:

$$v_{r\pm} = \frac{dr}{dt} = \frac{k_{\pm} V}{r} \frac{1}{\ln\left(\frac{r_o}{r_i}\right)} \qquad (2\text{-}2)$$

where $k_{\pm}$ is the ion's mobility.

The current which results from the collection of these charged particles is given by the following equation:

$$i_{\pm} = \frac{N_{\pm} k_{\pm} q \; 2\pi\ell}{\ln\left(\frac{r_o}{r_i}\right)} V(t) \qquad (2\text{-}3)$$

where $N_{\pm}$ is the charge number density and ℓ is the collector length.

The "+" and "-" subscripts are associated with the positive and negative charged particles, respectively. When a positive voltage V(t) is applied to the return electrode, positive ions having a mobility k_+ are collected resulting in a current i_+. The analogous explanation applies for negatively charged particles. The product term $N_{\pm} k_{\pm} q$ represents either the positive or negative electrical conductivity ($\sigma_{\pm}$) and thus, Equation (2-3) can be written as follows:

$$i_{\pm} = \frac{2\pi\ell}{\ln\left(\frac{r_o}{r_i}\right)} \sigma_{\pm} V(t) \qquad (2\text{-}4)$$

This expression describes the current collection when the condenser is operating in what is referred to as the "linear region." In this region of operation, only some of the ions in the atmospheric sample are being collected. The resulting current is seen to be proportional to ion conductivity and thus, operating the instrument in this region enables one to determine the positive and negative electrical conductivity values.

The operating condition for which all ions of one polarity entering the condenser are collected regardless of the initial velocity and radial point of entry is known as saturation. From an experimental point of view, it is important that the instrument is capable of operating in the saturation mode if one is to extract the ion mobility and charge number density information from the data. For the case of a Gerdien condenser descending on a stabilized parachute system, the axial flow velocity (<v>) through the condenser can be estimated from the radar fall data. This situation permits the saturation voltage to be specified as follows:

$$V_{s\pm} = \frac{\left(r_o^2 - r_i^2\right) \ln\left(\frac{r_o}{r_i}\right) \langle v \rangle}{2k_{\pm}\ell} \qquad (2\text{-}5)$$

The saturation voltage is the minimum voltage necessary to assure that all ions of one polarity entering the aspirator are collected by the inner electrode. When the instrument is operating in the saturation mode, the current of collected charged particles may be specified in the following equation:

$$i_{s\pm} = \pi(r_o^2 - r_i^2)N_{\pm}q\ \langle v \rangle \qquad (2\text{-}6)$$

The features of the linear region and the saturation region for the single ion mobility case are illustrated in Figure (2-2). The current-voltage characteristic shows the collection of positive ions, electrons and negative ions. Electrons are much more mobile than the negative ions and are saturated out at such a low voltage that the electron current causes an apparent step discontinuity at the origin. The remaining ions, both positive and negative, are collected in the manner illustrated. In the linear regions ① and Ⓐ, the slopes or current derivatives with respect to voltage ($di_{\pm}/dV$) are proportional to the ion conductivities as illustrated. Regions ② and Ⓑ depict the saturation regions and illustrate the dependence of the positive and negative ion currents on the product $N_{\pm}\langle v \rangle$.

The current-voltage relationship in Figure (2-2) is for the simplified case of ions of the same polarity having comparable mobility values; however, in actual operation it is possible to have different ion mobility species. This case will be covered in the following section.

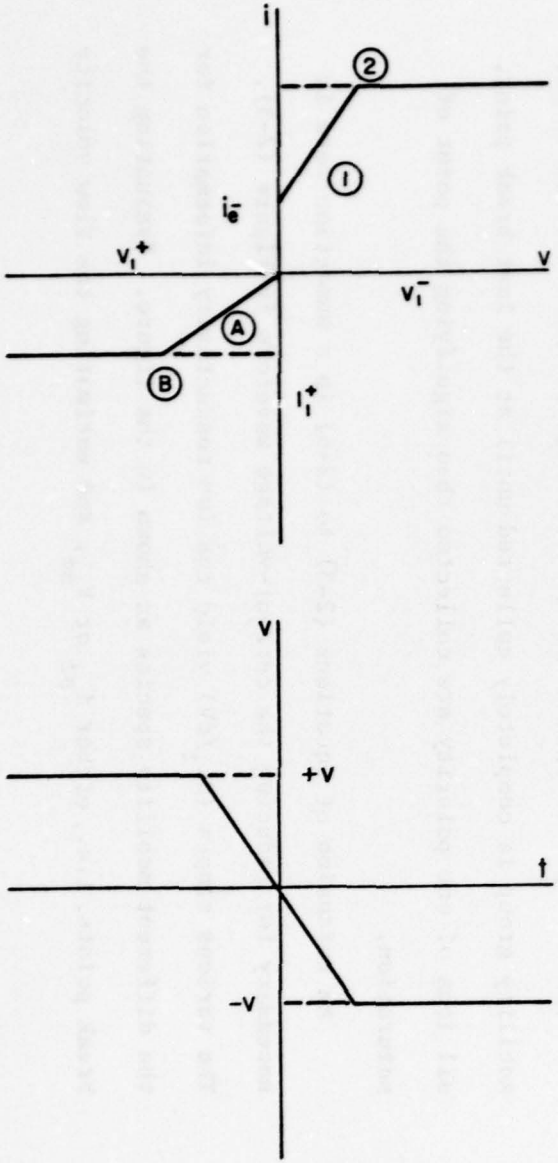

CURRENT-VOLTAGE CHARACTERISTIC FOR GERDIEN CONDENSER-SINGLE MOBILITY SPECIES

REGION	INFORMATION
①	N_-K_- } PROPORTIONAL TO $\frac{di}{dv}$
Ⓐ	N_+K_+ }
②	} SATURATION REGION, CURRENT PROPORTIONAL TO $(N_{\pm})(\langle V \rangle)$
Ⓑ	}

FIGURE (2-2)

2.2.2 Multiple Ion Mobility Species

If the theory of charged particle collection for the Gerdien condenser is extended to the case of ions of different mobilities, the current-voltage waveform is observed to display more structure. An illustration of this situation is shown in Figure (2-3). The figure illustrates the case of three different positive ion mobility groups and three distinct negative ion mobility groups in addition to electrons. The current-voltage relationshp shown actually represents the superposition of the current-voltage curves for each separate mobility group as illustrated previously in Figure (2-2). Again, the apparent discontinuity at the origin is attributed to the collection of electrons as explained previously. Moving from the origin to either the left or right, a series of slopes with break points are apparent. Each break point represents the voltage for which all charged particles within a certain mobility group have been collected. Each succeeding break point marks the voltage at which the next lower mobility group is completely collected until at the last break point, all ions of one polarity are collected thus signifying the point of saturation.

An extension of Equations (2-3) to (2-6) in a summation form is necessary for reducing the current-voltage waveform in Figure (2-3). The various slopes ($di_{\pm}/dV$) yield the ion conductivity information for the different mobility species as shown in the figure. Evaluating the break points, i.e., either $i_{s\pm}$ or $V_{s\pm}$, and estimating the flow velocity

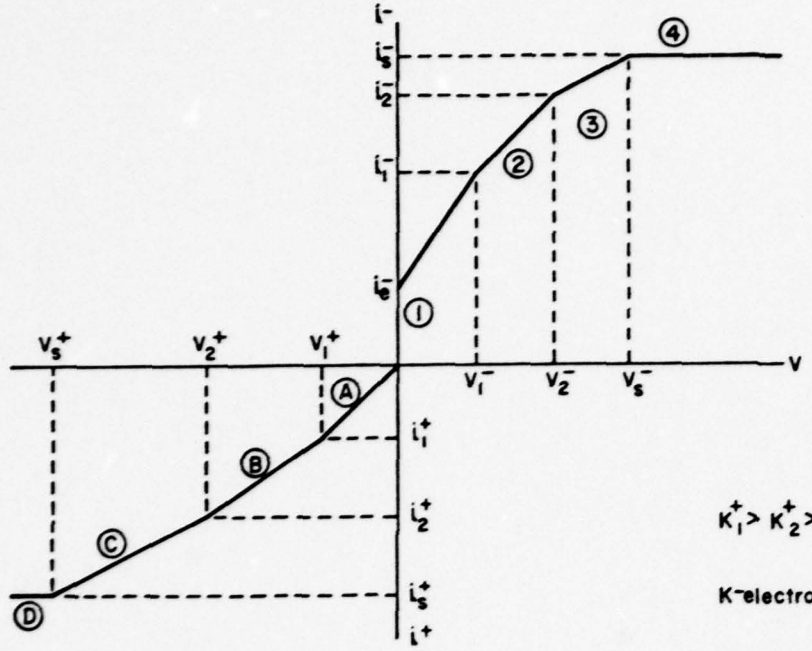

COLLECTION VOLTAGE WAVEFORM

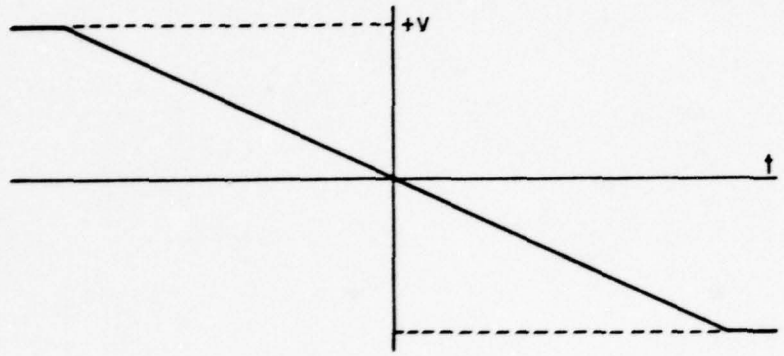

FIGURE (2-3)

CURRENT–VOLTAGE CHARACTERISTIC FOR GERDIEN CONDENSER

	REGION	INFORMATION (di/dv α to)
$K_1^+ > K_2^+ > K_3^+$	①	$(N_1^- K_1^- + N_2^- K_2^- + N_3^- K_3^-)$
K⁻electron >> K_1^-	②	$(N_2^- K_2^- + N_3^- K_3^-)$
$K_1^- > K_2^- > K_3^-$	③	$(N_3^- K_3^-)$
	④	(saturation)$(N_1^- + N_2^- + N_3^-)(\langle V \rangle)$
	Ⓐ	$(N_1^+ K_1^+ + N_2^+ K_2^+ + N_3^+ K_3^+)$
	Ⓑ	$(N_2^+ K_2^+ + N_3^+ K_3^+)$
	Ⓒ	$(N_3^+) K_3^+$
	Ⓓ	(saturation)$(N_1^+ + N_2^+ + N_3^+)(\langle V \rangle)$

<v> will in turn enable one to evaluate the different ion mobilities and number densities.

3. ELECTRICAL AND MECHANICAL DESIGN

3.1 Electrical Design

3.1.1 Introduction

The electronics for the Gerdien condenser include the internal power supply, the sweep voltage generator, the voltage-pulse rate converter and the telemetry system. The block diagram description of the Gerdien condenser electronics is shown in Figure (3-1).

A detailed analysis of the antenna system [Cuffin (1965)] and the operation of the power supply [ECOM Report No. 5144 (1967)], sweep voltage generator [Hale and Hoult (1965)], electrometer [Zimmerman (1971)], voltage-pulse rate converter [Pontano (1970)] and transmitter [Hale and Hoult 1965)] circuitry have been discussed previously in the designated references. A brief description of the function of these components will now be presented.

3.1.2 Power Supply

The power supply is a self-contained system utilizing four 1.25-volt rechargeable, nickel cadmium batteries. The batteries and associated converter circuitry (see Figure (3-2)) provide dc supply voltages of +110 V, +5 V and -20 V. The wiring diagram in Figure (3-3) shows the pin connections used with the power supply as well as the wiring connections and color code for the Gerdien condenser circuitry.

3.1.3 Sweep Voltage Generator

The collection or sweep voltage (Figure (3-4)) is actually applied to the return electrode with reference to the inner collecting electrode.

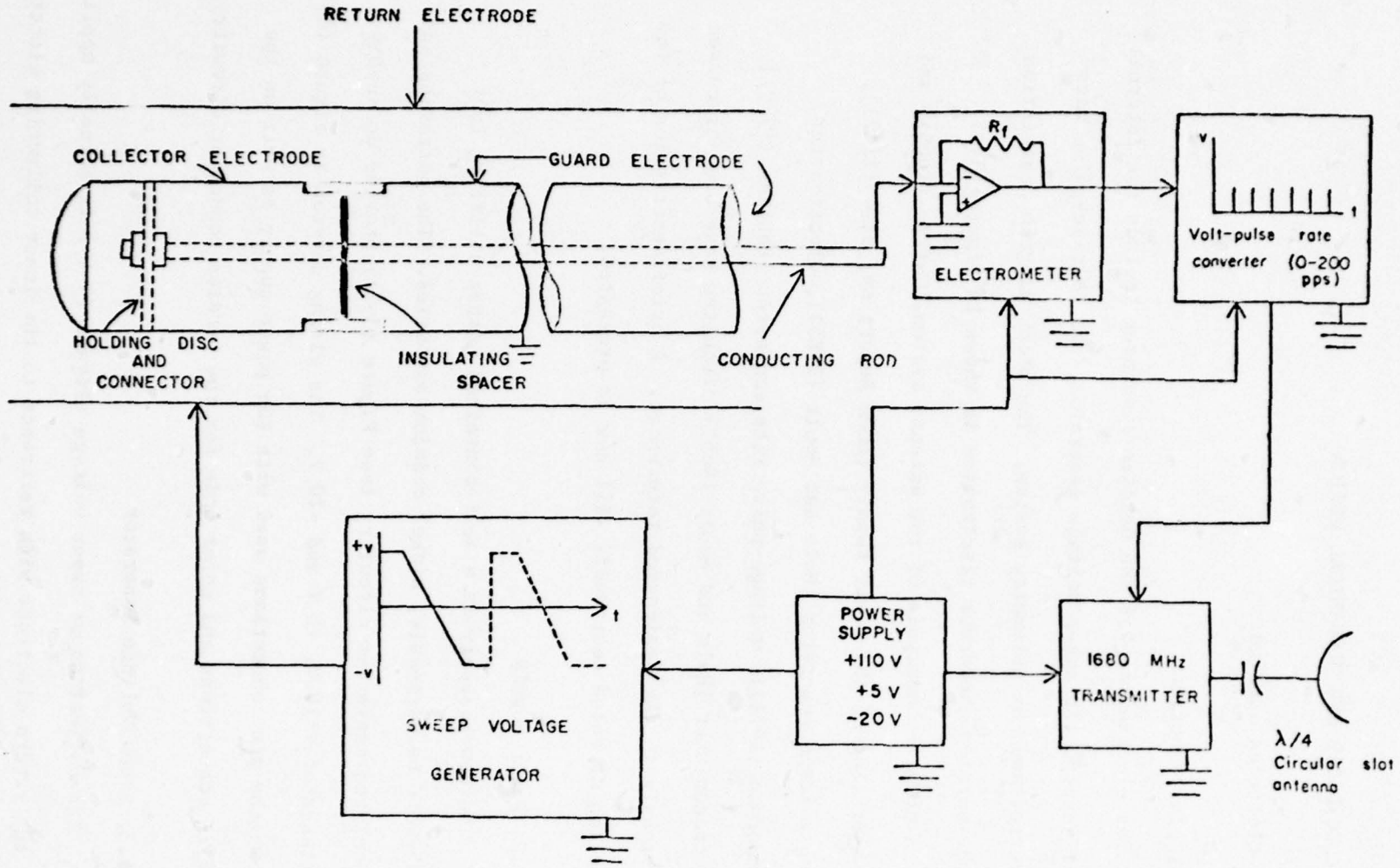

FIGURE (3-1) - Gerdien Condenser Block Diagram

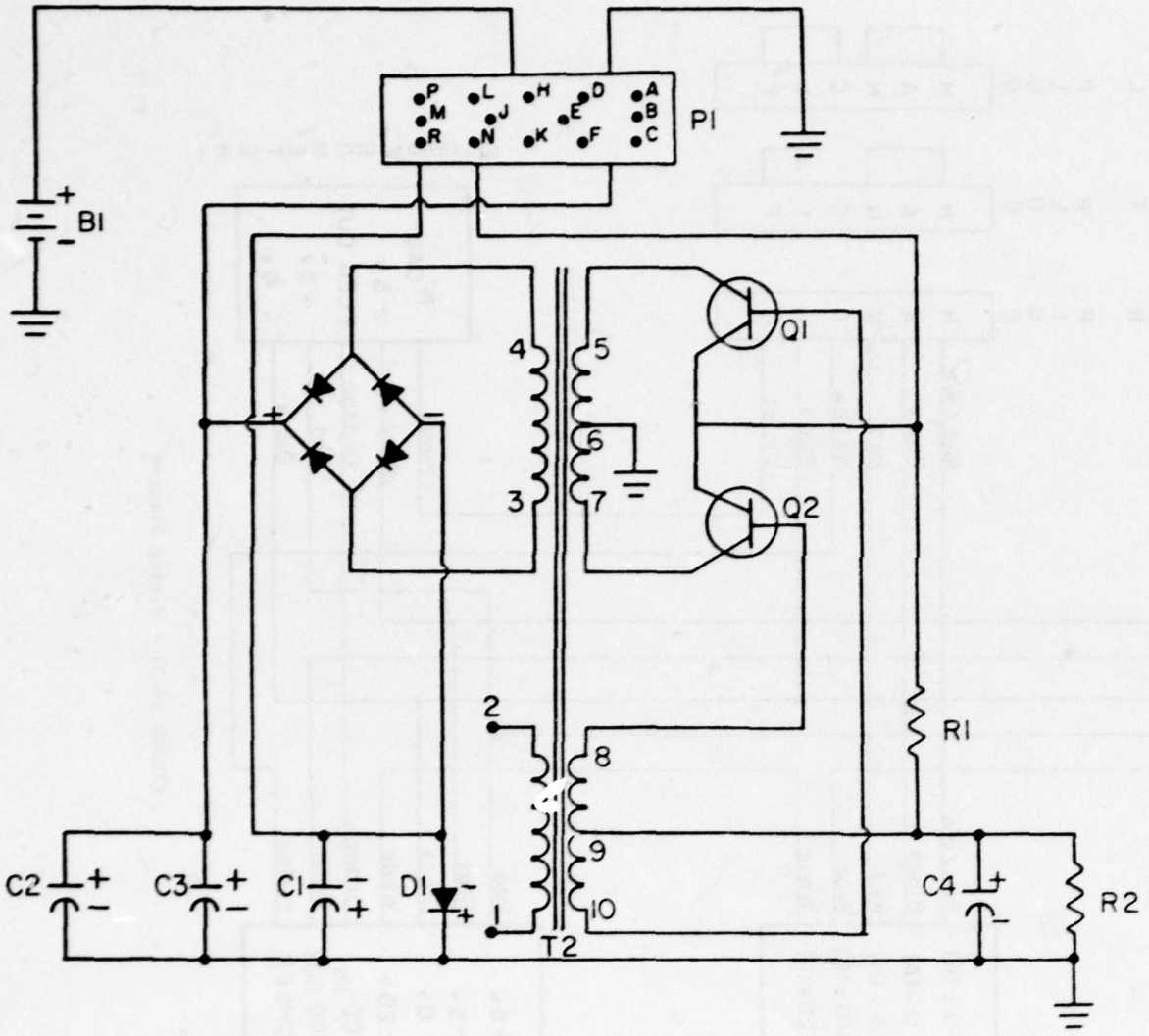

C1 = 50 MFD

C2 = C3 = 10 MFD

C4 = 1.0 MFD

R1 = 47

R2 = 470

Q1 = Q2 = 2N4057

D1 = IN2985

B1 = 6 v

T2 = Toroidal transistor power transformer (Thordarson TR283)

FIGURE (3-2) - Power Supply Circuit

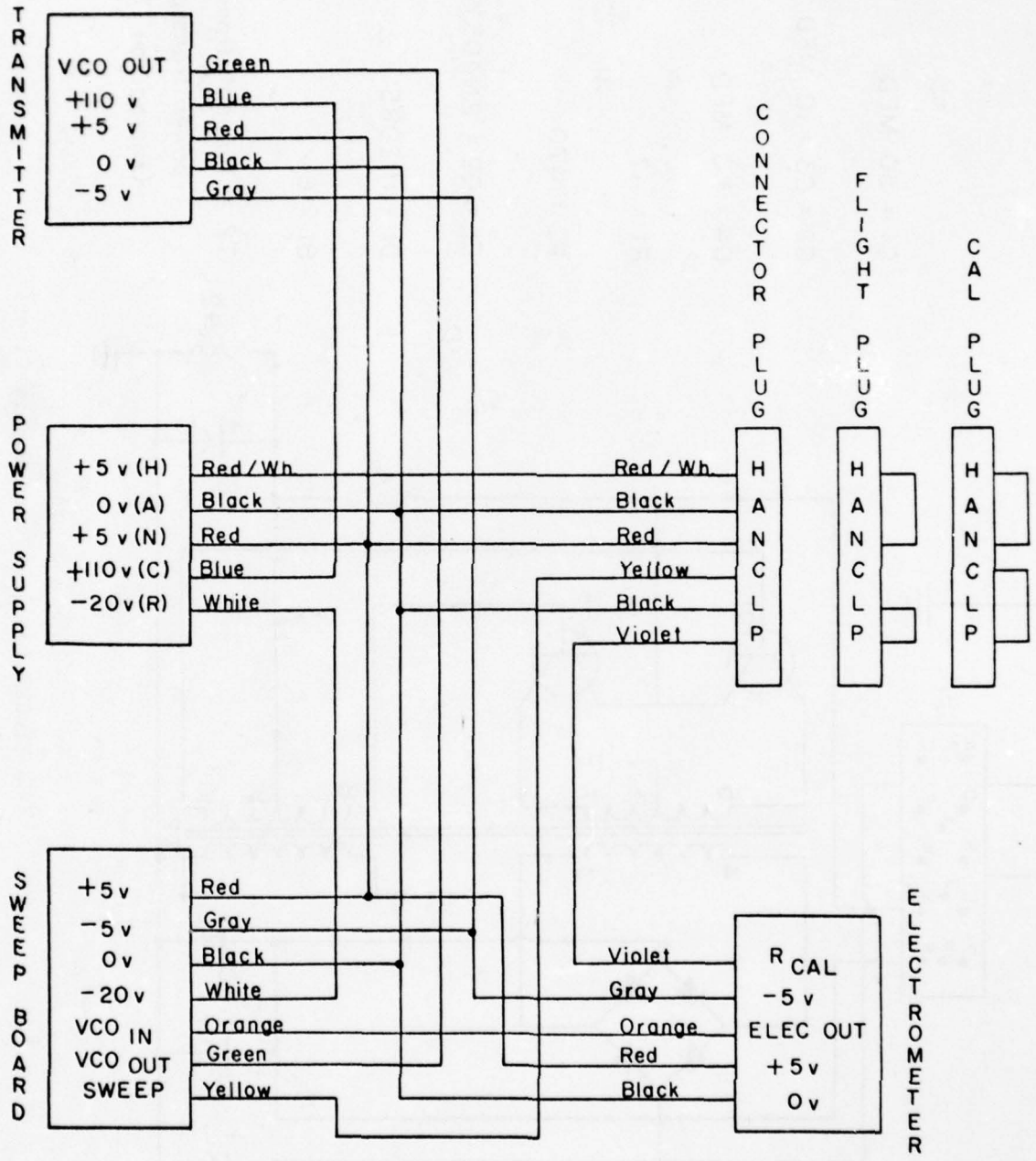

FIGURE (3-3) - Wiring Diagram

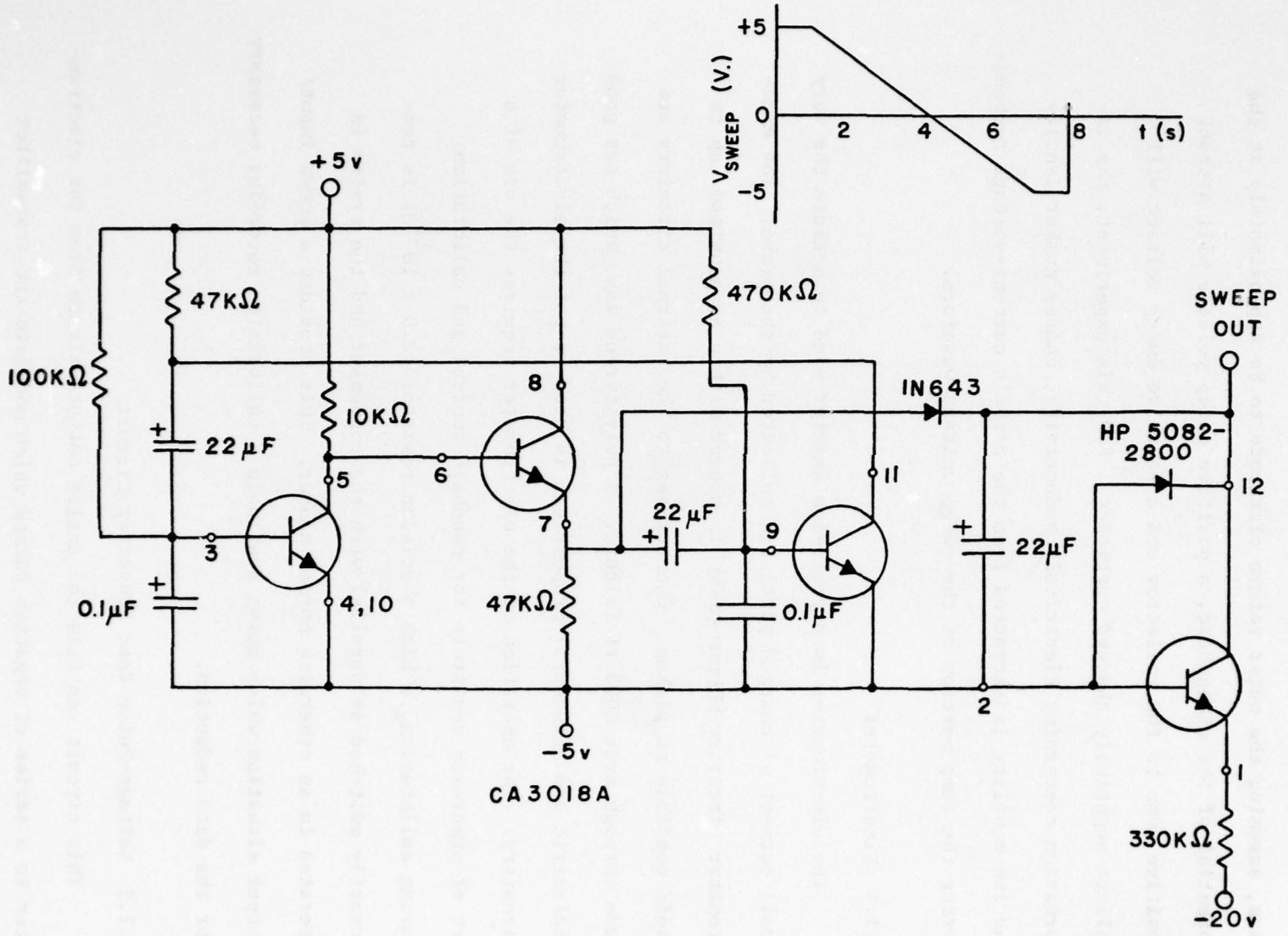

FIGURE (3-4) - Sweep Voltage Circuit

Thus, assuming the outer return electrode to be approximately at the potential of the atmosphere, a positive sweep voltage will attract positive ions to the collector and a negative sweep voltage will collect negatively charged particles. For this experiment, the information concerning electrical conductivity, charge number density and ion mobility is extracted from the probe's current-voltage response during the ramp portion of the sweep voltage waveform.

3.1.4 Electrometer

The electrometer is a precision ammeter used to measure the very small current of charged particles collected by the probe. The electrometer circuitry [Figure(3-5)] is housed within an aluminum cup to avoid possible rf pickup. Connections to the external circuitry are made through Erie E003 rf filters. A polystyrene wax, which has good dielectric and structural properties, is used to pot the electrometer circuitry. The operation of the electrometer requires the use of a set of precision resistors for feedback control and calibration. During calibration, a high precision resistor ($2.0 \times 10^{11}\Omega$) is temporarily switched in parallel with the condenser and the system is operated in an otherwise normal manner. This provides a known imput/output situation which makes available a calibration recording necessary for the data reduction.

3.1.5 Voltage-Pulse Rate Converter Circuit

This circuit converts the analog output voltage from the electrometer to a series of negative pulses which modulate the transmitter tube. For the particular circuit in Figure (3-6), the typical range

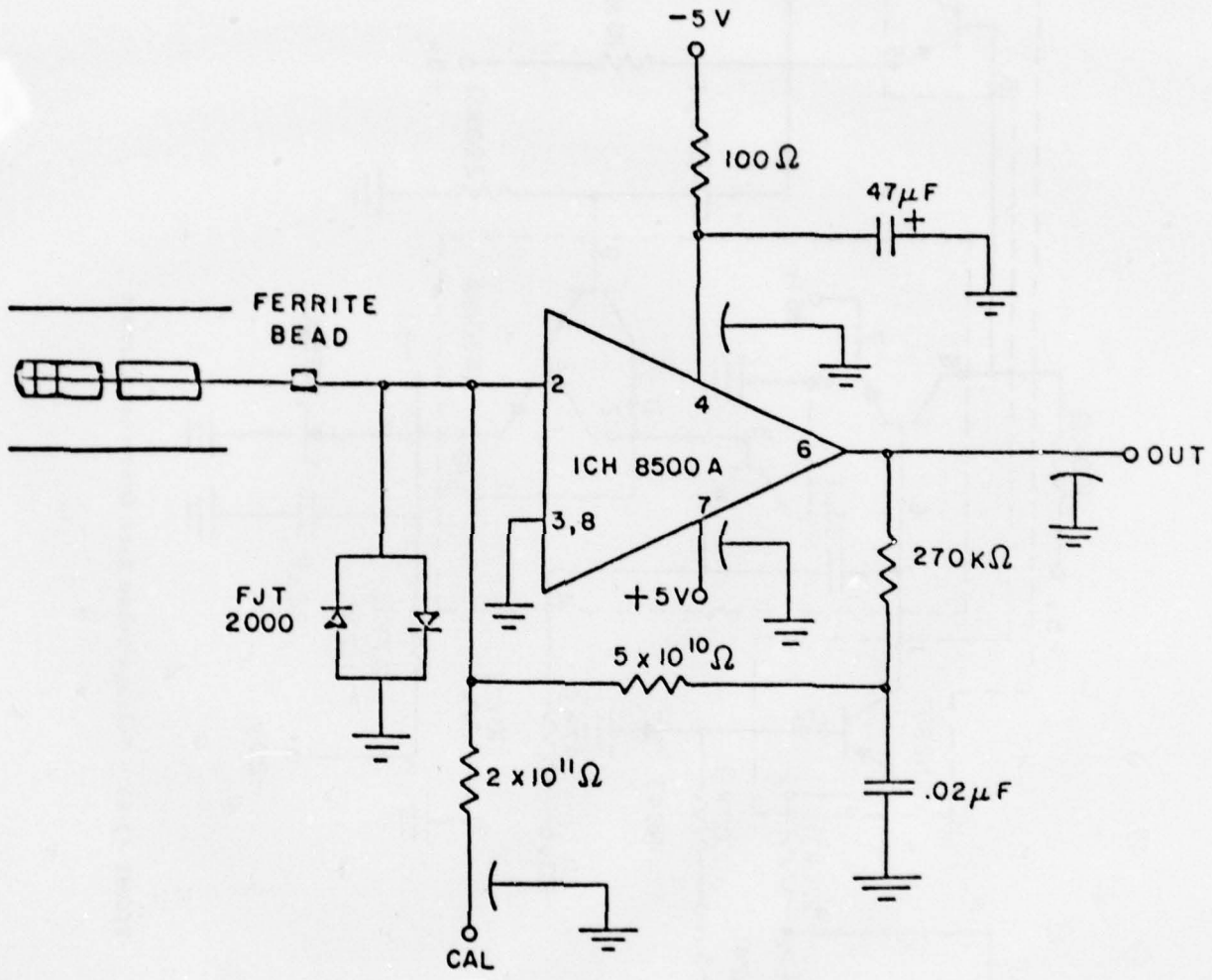

FIGURE (3-5) - Electrometer Circuit

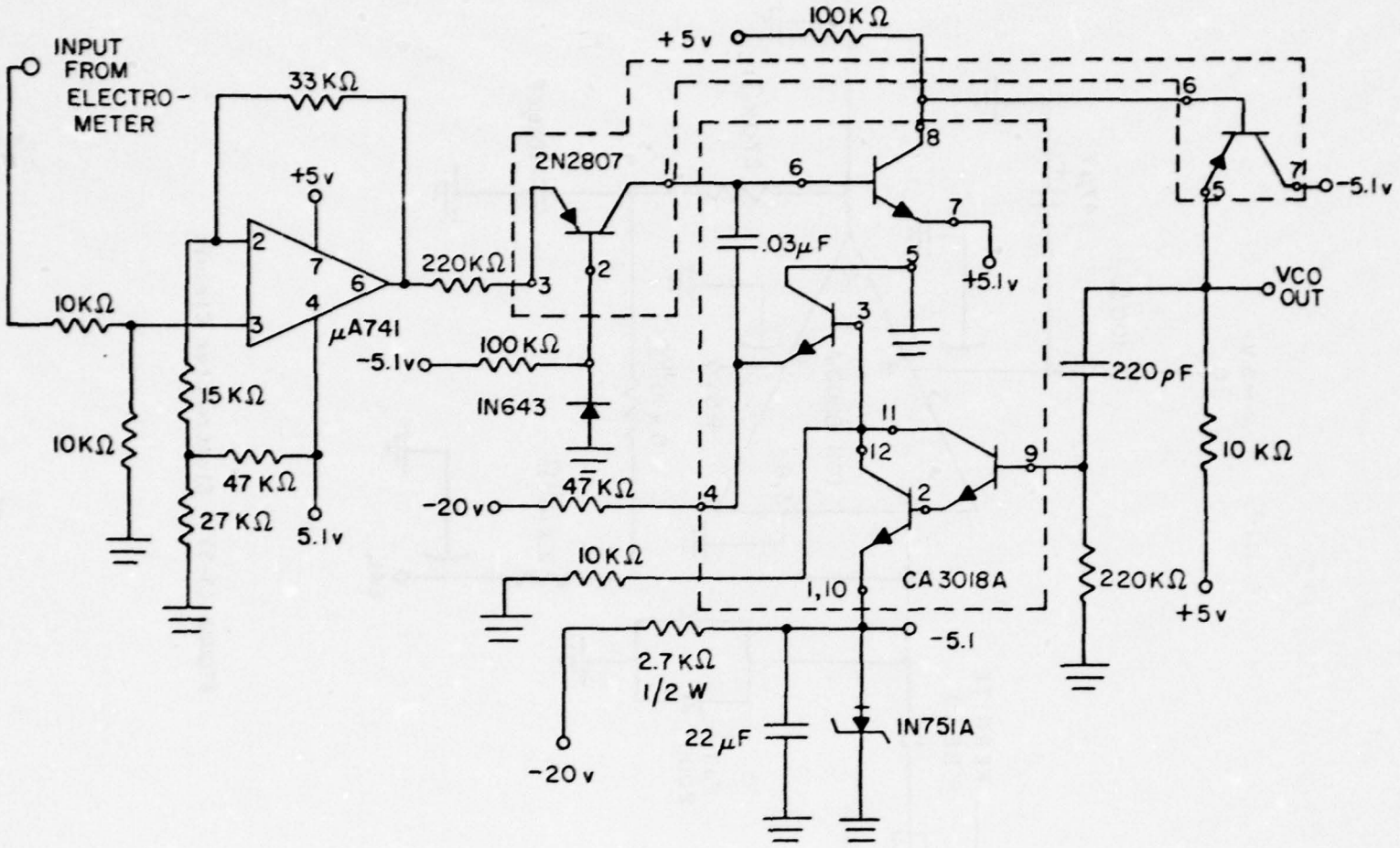

FIGURE (3-6) - Voltage-Pulse Rate Converter Circuit

of input voltages from -1.5 to +1.5 V corresponds linearly to pulse frequencies from approximately 0 to 200 pps. The output, which is capacitively coupled to the grid of the transmitter tube, alternately cuts the tube off thus producing a pulse modulated signal.

3.1.6 Transmitter and Antenna System

The transmitter circuit diagram is shown in Figure (3-7). The transmitter is an RCA 4048V3 microwave cavity device tunable to a frequency of 1680 MHz with some adjustment (±20 MHz) possible. The output of the transmitter tube is coupled to a $\frac{\lambda}{4}$ circular slot antenna.

3.2 Mechanical Design

A schematic of the Gerdien condenser is shown in Figure (3-8). The instrument has been designed for flight on a standard meteorological rocket system such as the Arcas rocket. The complete payload with base plate is 43.2 cm in length and weighs 2.18 kg. The diameter of the outer return electrode is 7.44 cm, while the collector diameter is 2.22 cm and is 6.35 cm in length.

The power supply forms the lower structure of the payload. A base plate for connecting the parachute lanyard is bolted to the bottom of the power supply. The entire power supply is potted with a polycel compound, thus providing electrical isolation as well as adding strength to the power supply structure. The antenna can, which is attached to the top of the power supply, contains the sweep voltage generator, voltage-pulse rate converter and transmitter circuitry. The electrometer is located as shown in Figure (3-8). A delrin spacer is used to interface the collector assembly to the antenna can. For

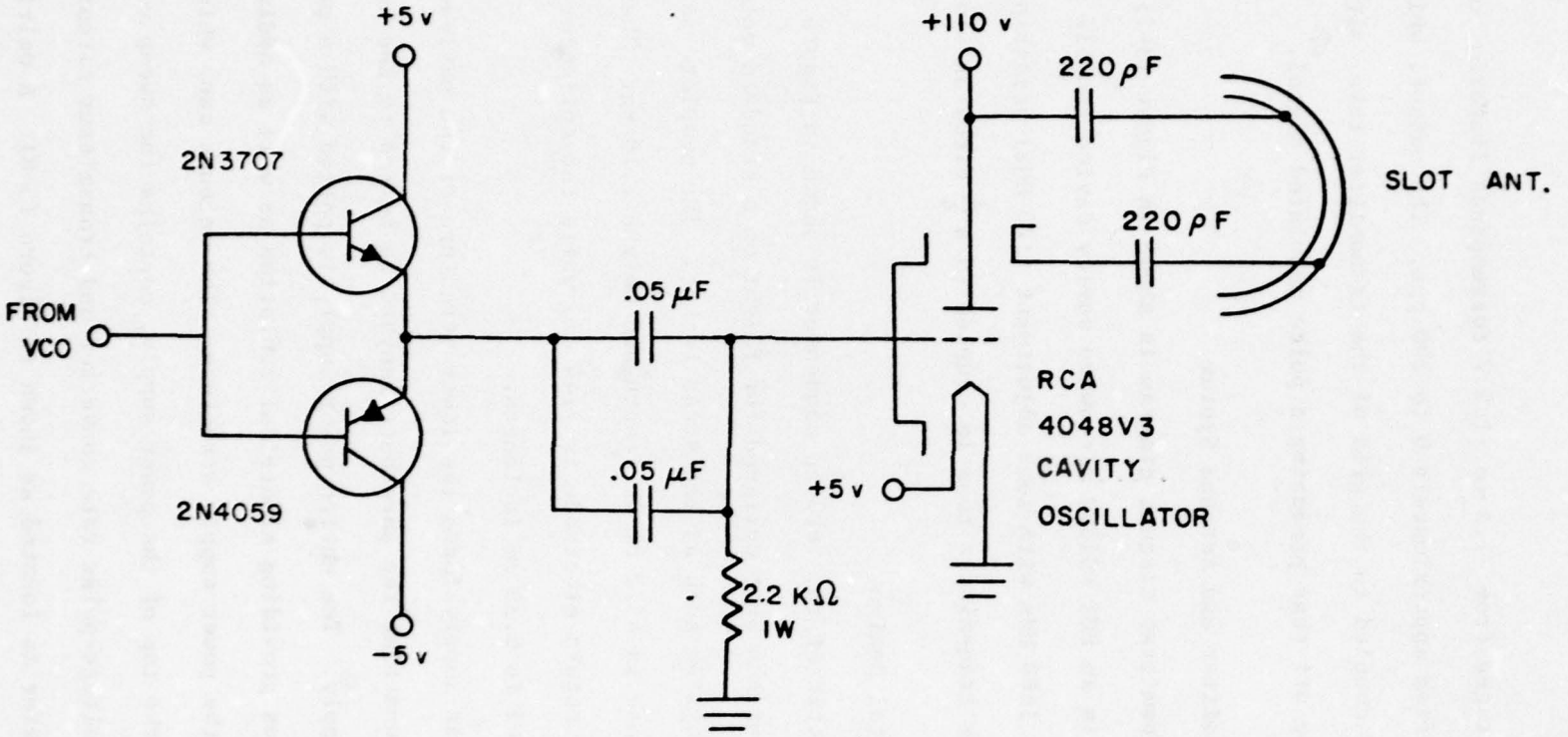

FIGURE (3-7) - Transmitter Circuit

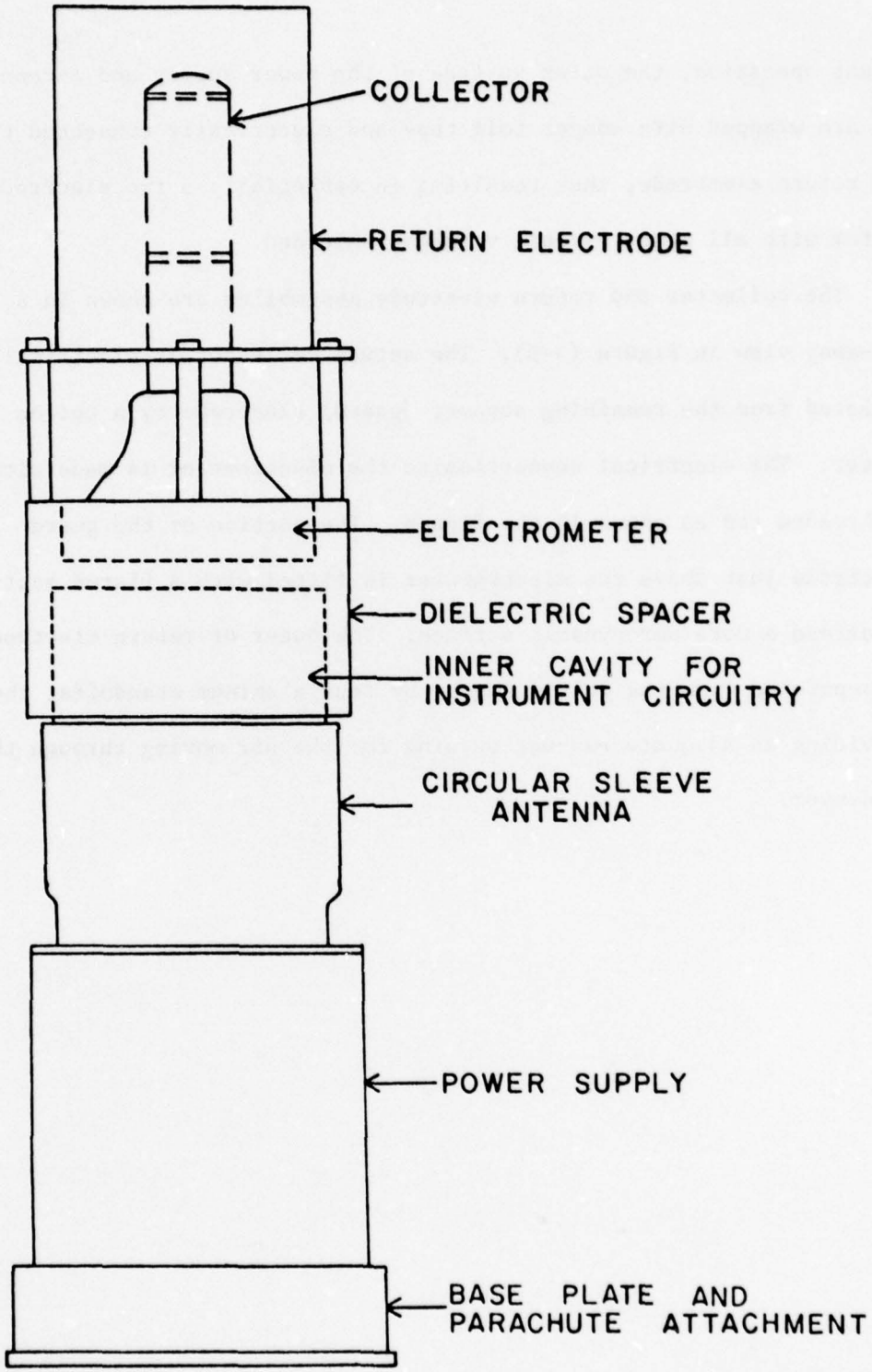
COLLECTOR
RETURN ELECTRODE
ELECTROMETER
DIELECTRIC SPACER
INNER CAVITY FOR INSTRUMENT CIRCUITRY
CIRCULAR SLEEVE ANTENNA
POWER SUPPLY
BASE PLATE AND PARACHUTE ATTACHMENT
GERDIEN CONDENSER

FIGURE (3-8)

flight operation, the outer surface of the power supply and antenna can are wrapped with copper foil tape and electrically connected to the return electrode, thus resulting in essentially a two electrode system with all other circuit voltages shielded.

The collector and return electrode assemblies are shown in a cut-away view in Figure (3-9). The actual collector is electrically isolated from the remaining support (guard) electrode by a teflon spacer. The electrical connection to the electrometer is made with a threaded rod as shown in the figure. The portion of the guard electrode just above the electrometer is fitted with a flared section to afford a more aerodynamic surface. The outer or return electrode is separated from the delrin spacer by four aluminum standoffs, thus providing an adequate exhaust opening for the air moving through the condenser.

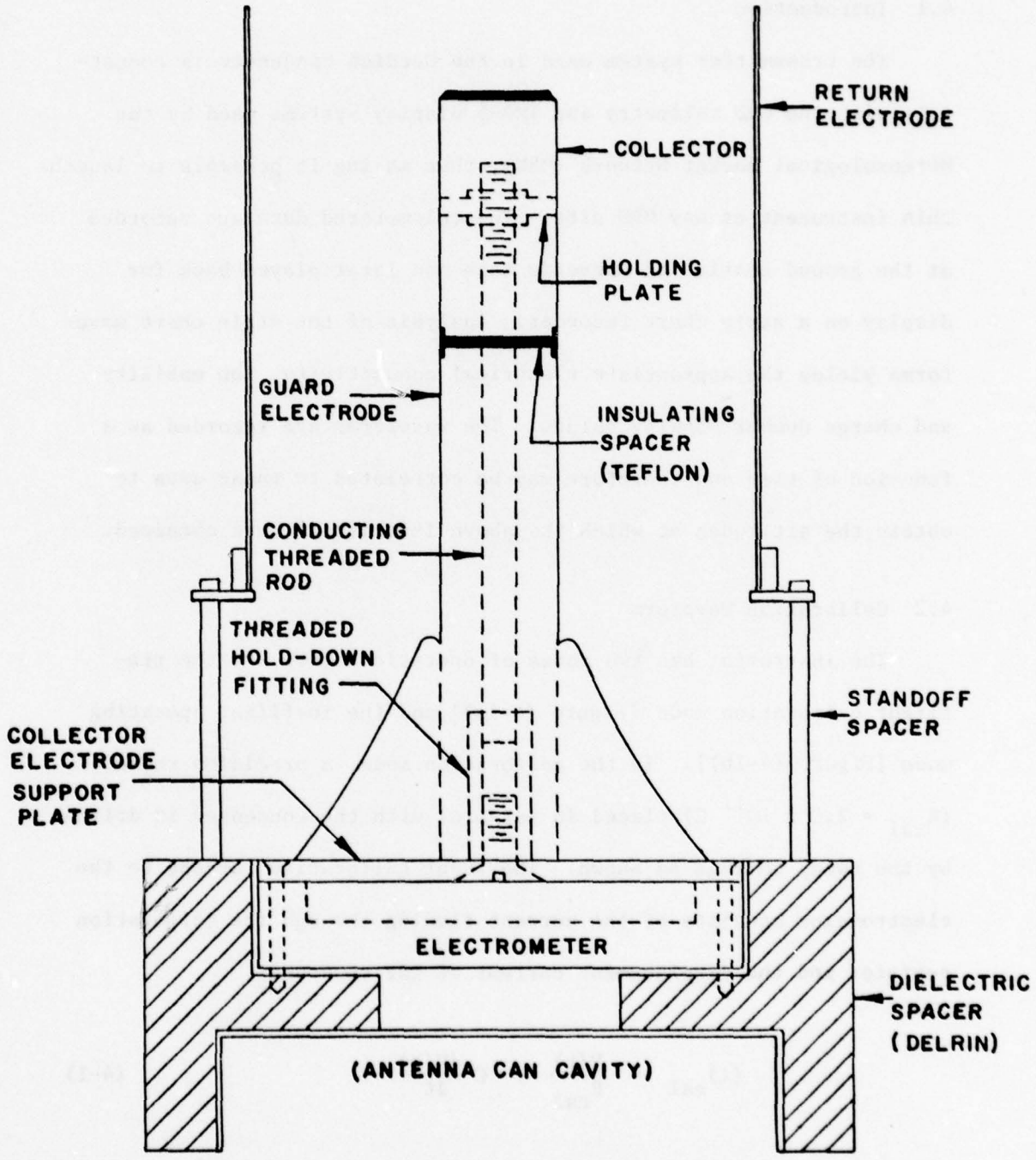

FIGURE (3-9) - Gerdien Condenser Collector Assembly

4. TELEMETRY/DATA ACQUISITION

4.1 Introduction

The transmitter system used in the Gerdien condenser is compatible with the GMD telemetry and TMQ-5 display systems used by the Meteorological Rocket Network (MRN), thus making it possible to launch this instrument at any MRN site. The telemetered data are recorded at the ground station on magnetic tape and later played back for display on a strip chart recorder. Analysis of the strip chart waveforms yields the appropriate electrical conductivity, ion mobility and charge number density values. The waveforms are recorded as a function of time and therefore may be correlated to radar data to obtain the altitudes at which the above information were obtained.

4.2 Calibration Waveform

The instrument has two modes of operation. They are the preflight calibration mode [Figure (4-1a)] and the in-flight operating mode [Figure (4-1b)]. In the calibration mode, a precision resistor ($R_{cal} = 2.0 \times 10^{11}\ \Omega$) placed in parallel with the condenser is driven by the sweep voltage as shown. The input calibration current to the electrometer consists of the current flowing through the calibration resistor and the displacement current of the condenser.

$$(i)_{cal} = \frac{V(t)}{R_{cal}} + C\,\frac{dV(t)}{dt} \qquad (4\text{-}1)$$

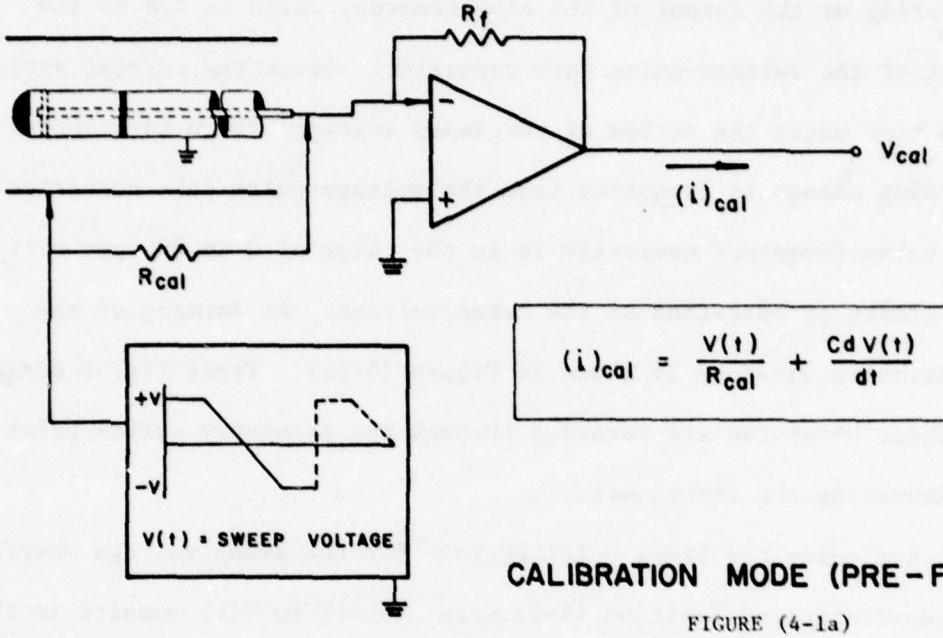

$$(i)_{cal} = \frac{V(t)}{R_{cal}} + \frac{Cd\,V(t)}{dt}$$

CALIBRATION MODE (PRE-FLIGHT)

FIGURE (4-1a)

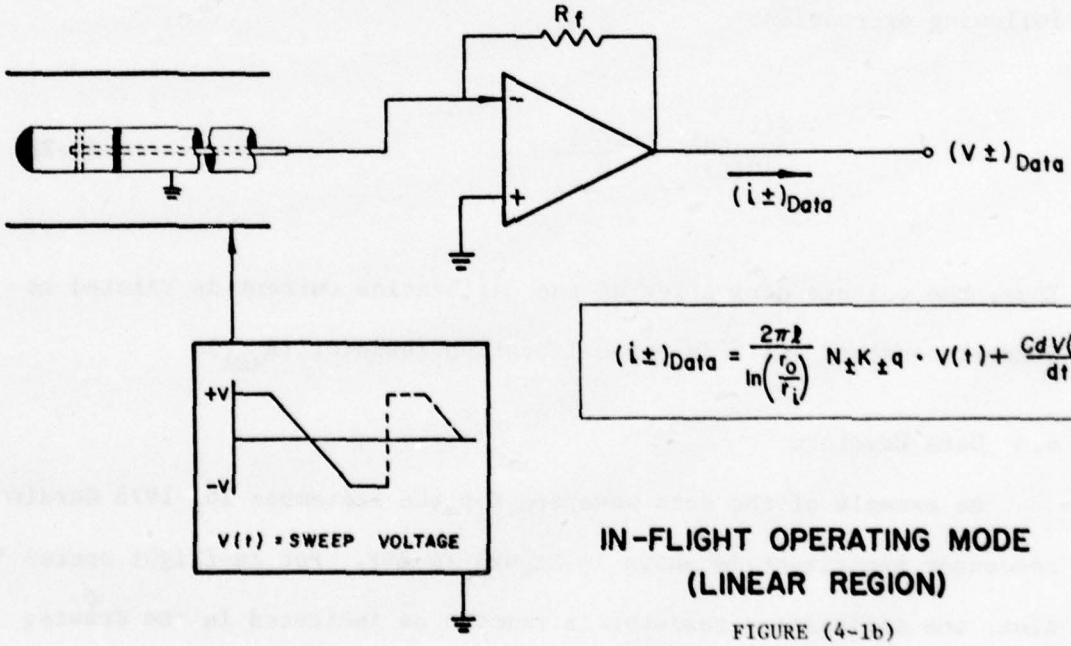

$$(i\pm)_{Data} = \frac{2\pi\ell}{\ln\left(\frac{r_o}{r_i}\right)} N_{\pm} K_{\pm} q \cdot V(t) + \frac{Cd\,V(t)}{dt}$$

IN-FLIGHT OPERATING MODE (LINEAR REGION)

FIGURE (4-1b)

The result of this current is the calibration voltage (V_{cal}) appearing at the output of the electrometer, which is fed to the input of the voltage-pulse rate converter. Since the current varies with time under the action of the sweep voltage, there is a corresponding change in frequency from the voltage-pulse rate converter. The pulse frequency nominally is in the range of 0 to 200 pps over the limits of operation of the sweep voltage. An example of the calibration waveform is shown in Figure (4-2a). Typically, a series of these waveforms are recorded through the telemetry system prior to launching the instrument.

Excluding the break point regions for the sweep voltage waveform, the derivative of Equation (4-1) with respect to V(t) results in the following expression:

$$\frac{d(i)_{cal}}{dV(t)} = \frac{1}{R_{cal}} \qquad (4\text{-}2)$$

Thus, the voltage derivative of the calibration current is related to a known constant which is the calibration resistor (R_{cal}).

4.3 Data Waveform

An example of the data waveform for the September 26, 1975 Gerdien condenser experiment is shown in Figure (4-2b). For in-flight operation, the calibration resistor is removed as indicated in the drawing [Figure (4-1b)]. The input current to the electrometer while in flight consists of the current due to charged particle collection and the condenser displacement current. Using Equation (2-4), the

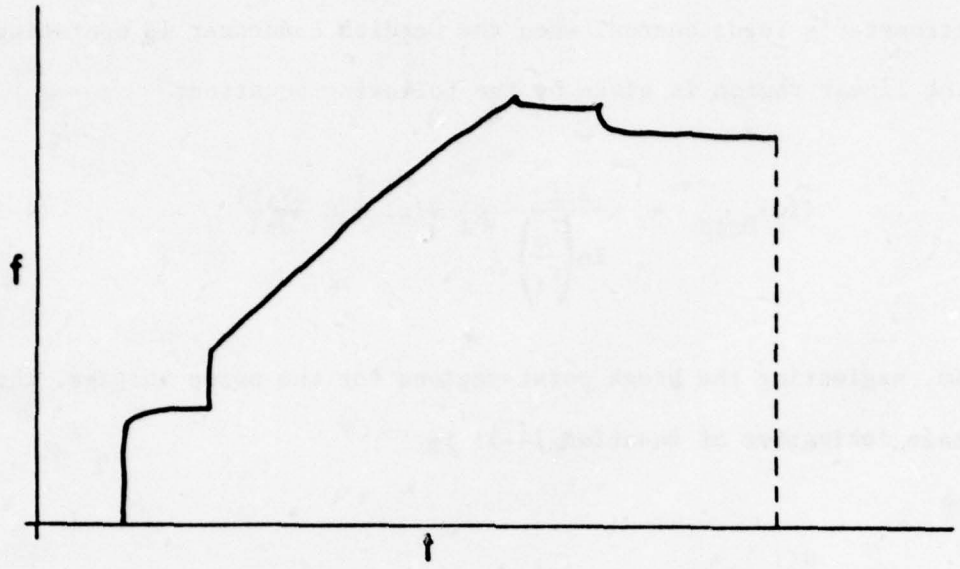

RECEIVED CALIBRATION WAVEFORM

FIGURE (4-2a)

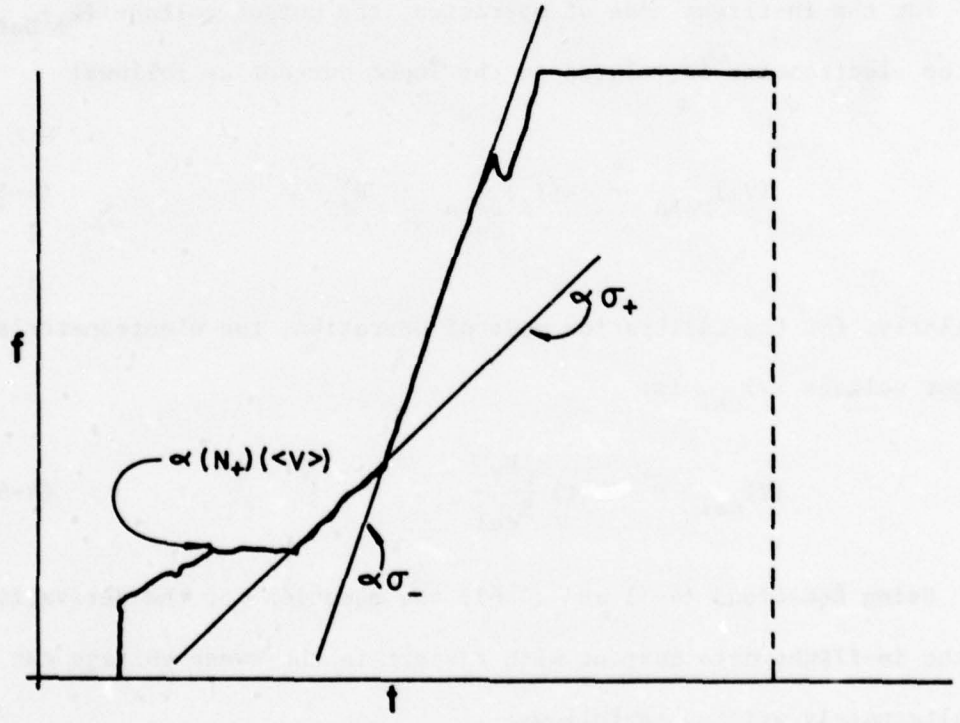

RECEIVED DATA WAVEFORM

FIGURE (4-2b)

electrometer's input current when the Gerdien condenser is operating in the linear region is given by the following equation:

$$(i_{\pm})_{Data} = \frac{2\pi\ell}{\ln\left(\frac{r_o}{r_i}\right)} \sigma_{\pm} V(t) + C \frac{dV(t)}{dt} \qquad (4\text{-}3)$$

Again, neglecting the break point regions for the sweep voltage, the voltage derivative of Equation (4-3) is:

$$\frac{d(i_{\pm})_{Data}}{dV(t)} = \frac{2\pi\ell}{\ln\left(\frac{r_o}{r_i}\right)} \sigma_{\pm} \qquad (4\text{-}4)$$

4.4 Data Reduction

For the in-flight mode of operation, the output voltage $(V_{\pm})_{Data}$ of the electrometer is related to the input current as follows:

$$(V_{\pm})_{Data} = -(i_{\pm})_{Data} \cdot R_f \qquad (4\text{-}5)$$

Similarly, for the calibration made of operation, the electrometer's output voltage $(V)_{cal}$ is:

$$(V)_{cal} = -V(t) \frac{R_f}{R_{cal}} \qquad (4\text{-}6)$$

Using Equations (4-5) and (4-6), the equation for the derivative of the in-flight data current with respect to the sweep voltage can be alternately written as follows:

$$\frac{d(i_{\pm})_{Data}}{dV(t)} = \frac{1}{R_{cal}} \frac{\left(\frac{dV_{\pm}}{dt}\right)_{Data}}{\left(\frac{dV}{dt}\right)_{cal}} \qquad (4\text{-}7)$$

Combining Equations (4-2), (4-4) and (4-7) yields the expression which may be used in the linear region to determine electrical conductivity:

$$\sigma_{\pm} = \frac{\ln\left(\frac{r_o}{r_i}\right)}{2\pi\ell\, R_{cal}} \frac{\left(\frac{dV_{\pm}}{dt}\right)_{Data}}{\left(\frac{dV}{dt}\right)_{cal}} \qquad (4\text{-}8)$$

Since the voltage-pulse rate converter linearly converts the electrometer output to a pulse frequency for modulating the transmitter, Equation (4-8) can be written in terms of the transmitter's pulse frequency as follows:

$$\sigma_{\pm} = \frac{\ln\left(\frac{r_o}{r_i}\right)}{2\pi\ell\, R_{cal}} \frac{\left(\frac{df_{\pm}}{dt}\right)_{Data}}{\left(\frac{df}{dt}\right)_{cal}} \qquad (4\text{-}9)$$

Equation (4-9) is used to extract the electrical conductivity information from the telemetered data waveforms. An example of how the waveform is scaled to obtain the electrical conductivity values is shown in Figure (4-2b).

The ion mobility and charge number density are obtained from the data waveform by evaluating either the saturation voltage ($V_{s\pm}$) or

the saturation current (i_{st}). Figure (4-2b) illustrates the point of saturation (break point) for the positive ion current. In this example, only one break point is present in the positive ion curve, thus indicating that one positive ion mobility group was completely collected by the instrument. For the portion of the data waveform representing the collection of negatively charged particles, the apparent break point observed is not due to saturation but rather is associated with the break in the sweep voltage. The absence of any saturation break point perhaps indicates that the collection voltage was not large enough to collect all of the negative ions moving through the aspirator.

5. MEASUREMENTS AND DISCUSSION

5.1 Introduction

The initial Gerdien condenser flights were conducted at White Sands Missile Range (WSMR), New Mexico (32°N, 106°W) on July 15, 1975 at 0618 MST and September 26, 1975 at 0600 MST. The same instrument was flown on both of these occasions. Launch parameters for these two experiments, as well as for two previous early morning blunt probe flights conducted at WSMR [Mitchell (1973); Mitchell and Hale (1973)], are listed in Table (5-1). The two blunt probe experiments measured only electrical conductivity.

5.2 Data

The positive ion conductivity profiles for the Gerdien condenser and blunt probe experiments are shown in Figure (5-1). These four curves represent the most recent early morning profiles (solar zenith angles in the range of 90° to 53°) for the WSMR launch site.

Although the data were obtained over approximately a four-year period, variations in ionization should be relatively small in the region below 60 km where the production of ions is primarily attributed to galactic cosmic rays. This is demonstrated by the consistency of the conductivity values at 30 km, thus indicating relatively small differences associated with seasonal and diurnal variations as well as different measurement techniques.

For the Gerdien condenser flights, the positive ion mobility data and corresponding charge number densities are plotted in Figures (5-2) and (5-3), respectively. The shaded and light circles indicate that two distinct ion mobility groups were measured on September 26, with the

TABLE(5-1)

PARAMETERS FOR WSMR MORNING ROCKET LAUNCHES

Date	Time (MST)	Solar Zenith Angle (°)	Experiment	Apogee (km)
June 9, 1971	0809	53	Blunt Probe	79
July 28, 1971	0705	68	Blunt Probe	78
July 15, 1975	0618	75	Gerdien Condenser	69
Sept. 26, 1975	0600	90	Gerdien Condenser	75

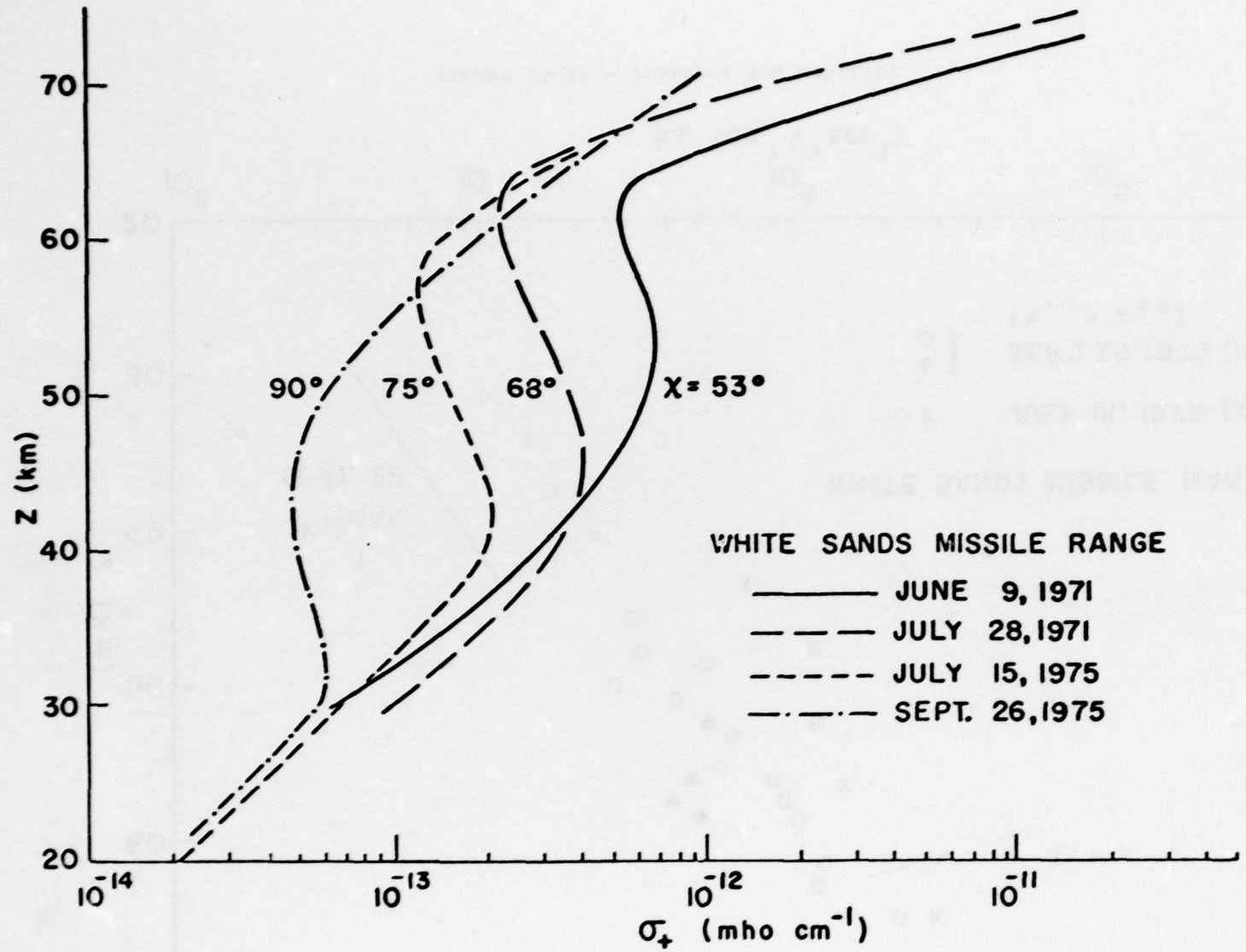

FIGURE (5-1) - Positive Ion Conductivity (Composite)

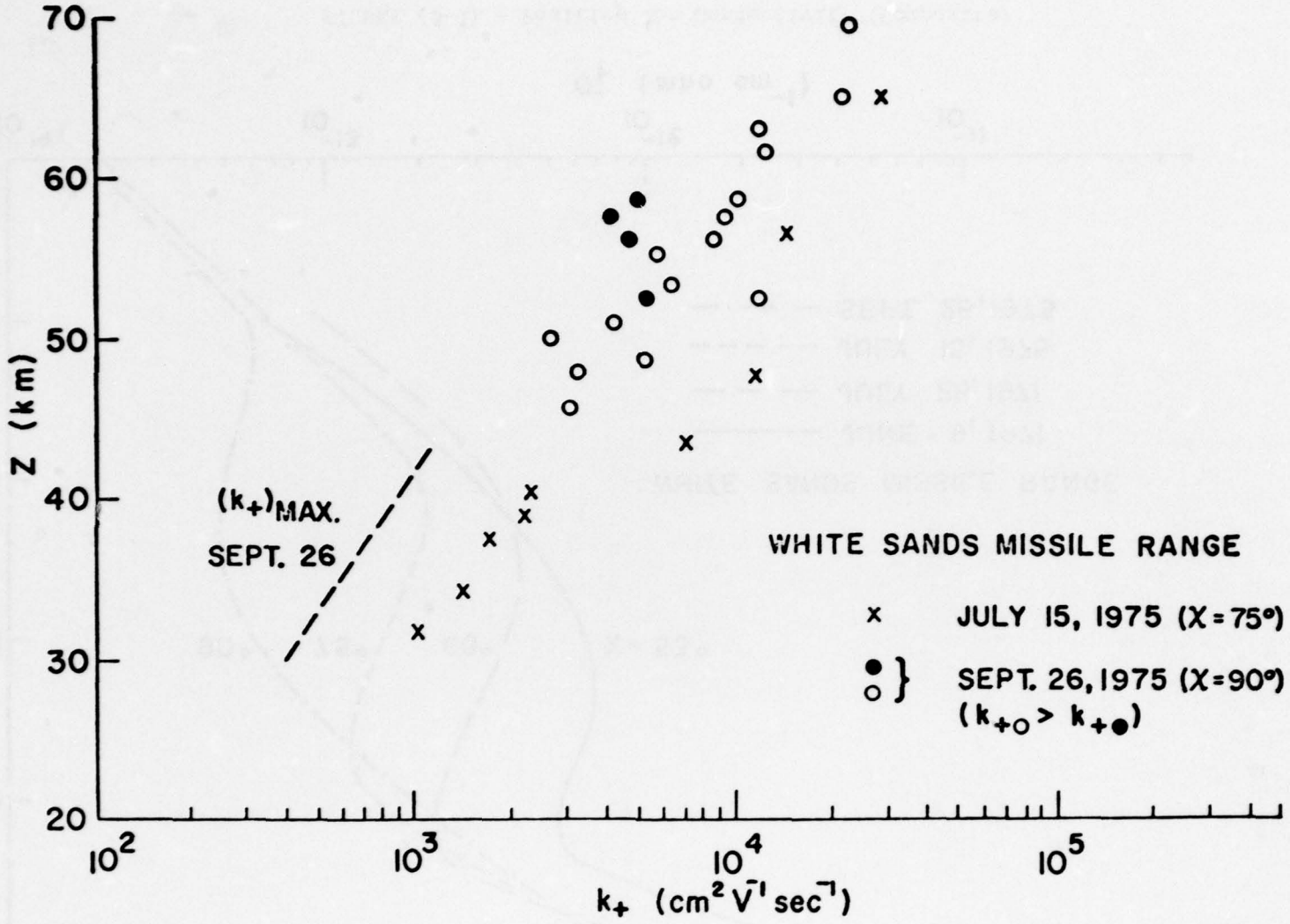

FIGURE (5-2) - Positive Ion Mobility

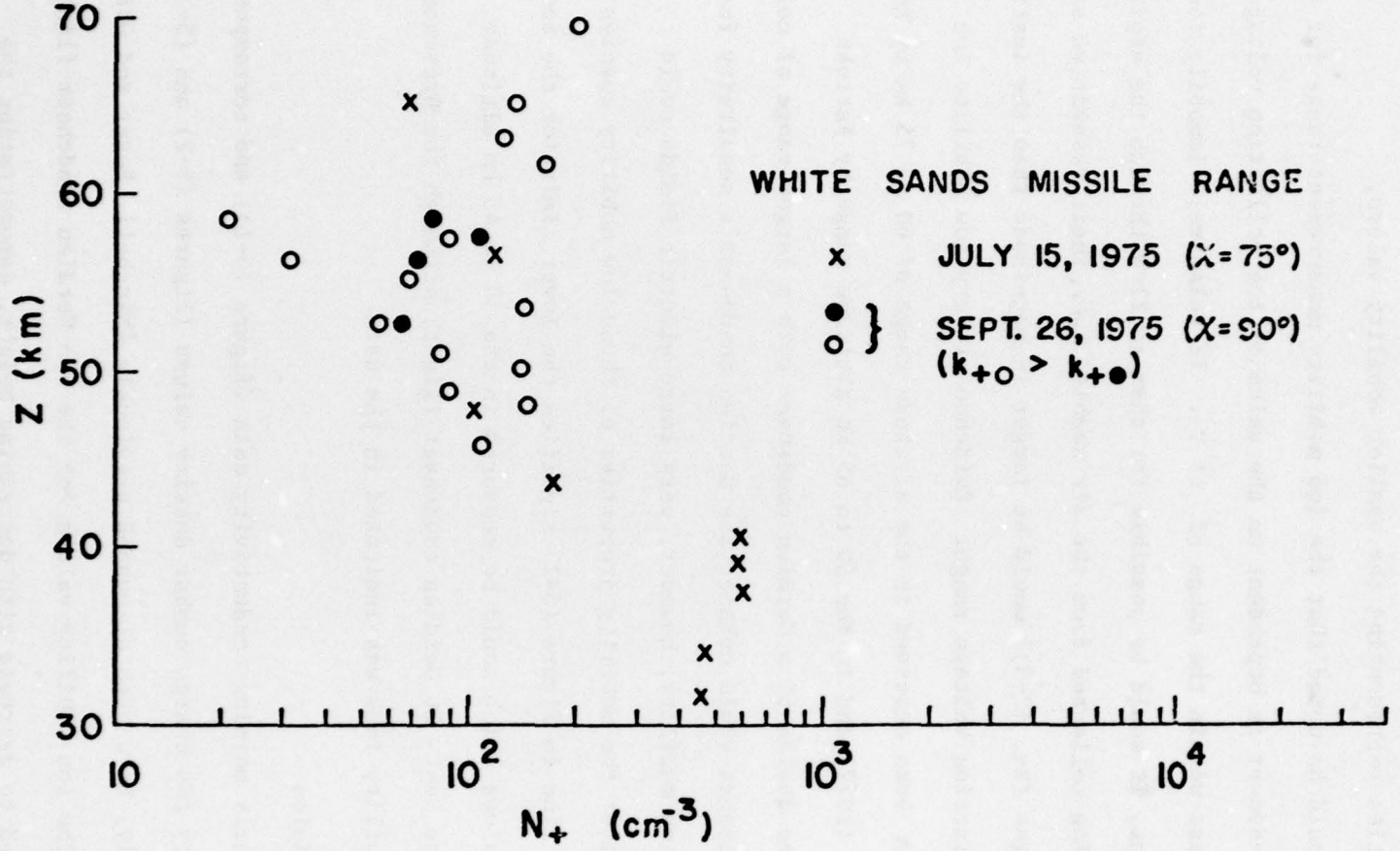

FIGURE (5-3) - Positive Ion Charge Number Density

shaded circles representing the smaller mobility values.

It should be noted that the ion mobility measurement range for the Gerdien condenser is dependent on the value of the collection voltage (in this case within the range of ±5 V). If relatively immobile ions were present, it would be possible for them to flow through the aspirator without being collected from the air sample, i.e., their respective saturation voltages (Eq. (2-5)) would be larger in magnitude than the instrument's collection voltage range. Evidence of very low mobility ion species has been observed in the altitude range of 60 to 75 km by Rose and Widdel (1972) and in the 50 to 65 km altitude range by Farrokh (1975). The design of a Gerdien condenser with a larger range of collection voltages would enhance the Gerdien condenser's sensitvity for measuring ion mobility; however, very large electric fields could possibly alter the mobility properties of these low mobility species. The dashed line in Figure (5-2) signifies the lower limit for the ion mobility values which could be measured in the 30 to 45 km altitude range on the Sept. 26 Gerdien condenser flight, although the presence of smaller mobility ions was indicated in the data.

5.3 Discussion

The early morning conductivity data (Figure (5-1)) and corresponding ion mobility and charge number density values (Figures (5-2) and (5-3) respectively) have been discussed previously [Mitchell, Sagar and Olsen (1977)]. The ion mobility values for the two Gerdien condenser flights are observed to decrease with decreasing height, demonstrating the altitude dependence of this parameter. A change in ion mobility with respect to altitude is particularly evident between 40 and 45 km,

suggesting a transition in ion mobility groups. A similar observation was reported by Rose and Widdel (1972). It should be noted that this transition region also corresponds to the region where Arnold, Krankowsky and Marien (1977) observe a change in positive ion composition from proton hydrates (at higher altitudes) to non-proton hydrates (at lower altitudes).

Of noted interest is the observed buildup in positive ion conductivity, particularly in the 35 to 55 km altitude region where the production mechanism for positive ions (galactic cosmic ray ionization) has little diurnal or seasonal dependence [Velinov (1968)]. Conductivity enhancements of at least an order of magnitude were observed between 45 and 50 km, corresponding to a change in solar zenith angle from 90° to 53°. A conductivity change of this size is not believed to be explainable by a change in ionization, and recent studies of temperature-dependent variations for midday positive conductivity values demonstrate at most a change of 4.6%/°K for this altitude region [Cipriano, Hale and Mitchell (1974)].

A comparison of the ion mobility data for the two Gerdien condenser experiments indicates that the values for July 15 (χ = 75°) are approximately a factor of two larger than the corresponding values for September 26 (χ = 90°), while the corresponding ion number density values are comparable. Thus, the buildup in positive ion conductivity observed between the change in morning solar zenith angle from 90° to 75° appears to be primarily associated with an increase in ion mobility. Such behavior is thought to be explainable by a photodissociation process resulting in the formation of smaller, more mobile ions.

The solar dependence for positive conductivity is better demon-

strated in Figure (5-4) where the secant of the solar zenith angle (χ) is plotted as a function of conductivity for different altitudes. Electrical conductivity data obtained later in the morning ($\chi = 44°$) showed no further enhancement in value, thus suggesting that this phenomenon is limited to the early morning period.

Finally, it should be noted that the two Gerdien condenser flights present a somewhat limited picture of the early morning ionization processes since they correspond to solar zenith angles of 90° and 75°. As demonstrated in Figure (5-1), a continued positive conductivity buildup was observed through a solar zenith angle of 53°, during which no corresponding ion mobility and number density measurements were made. The mechanism (ion mobility and/or number density) for this extended conductivity buildup is thus unknown, and is proposed as a subject for further study. Also, recalling that the data used in this report covered a four-year period, a further study should be conducted using measurements obtained over a relatively shorter time frame (preferably on the order of days) and also repeated for periods of different solar activity.

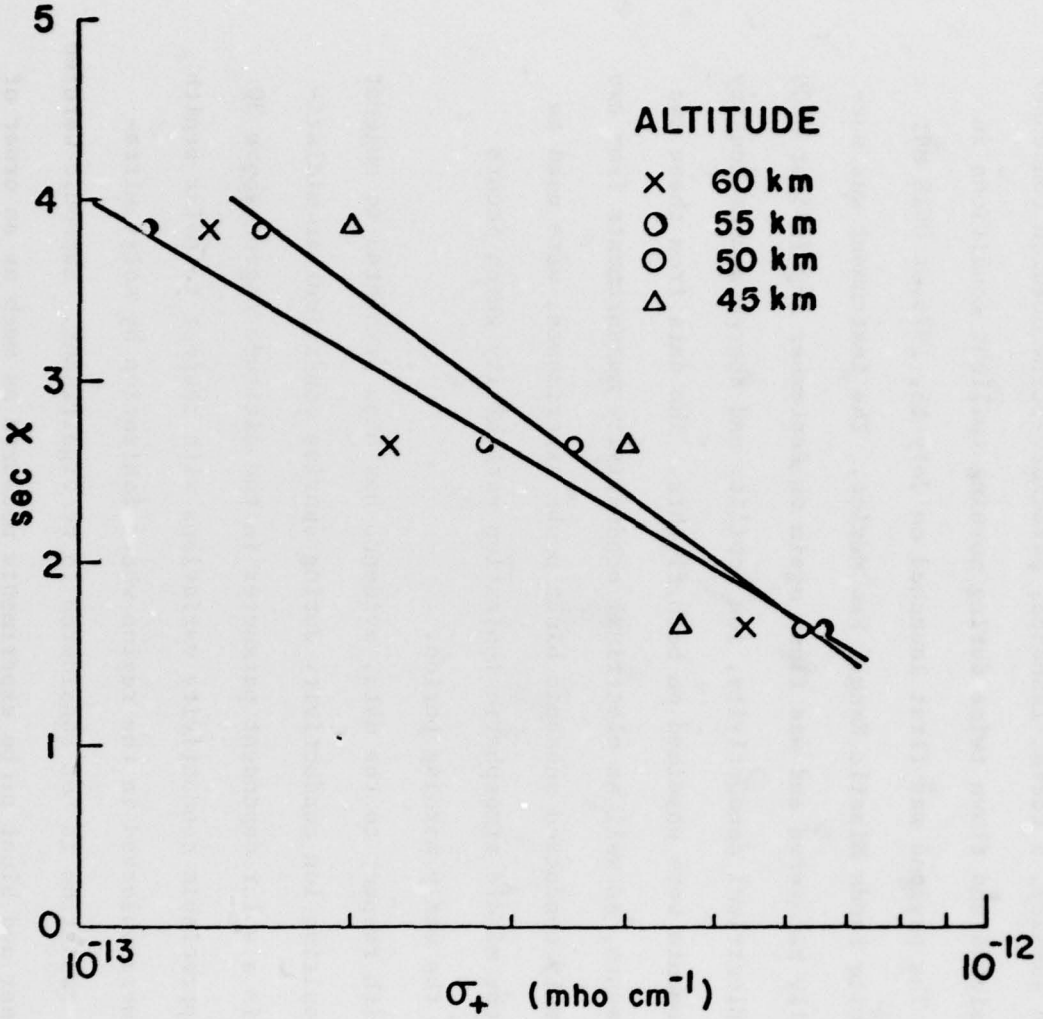

FIGURE (5-4) - Secant of Solar Zenith Angle Versus Positive Conductivity

6. CONCLUSIONS AND RECOMMENDATIONS

6.1 Conclusions

In summary, a rocket-launched, parachute-borne Gerdien condenser was designed and flown twice during morning twilight conditions in 1975. The payload was first launched on July 15, 1975 at 0618 MST from White Sands Missile Range, New Mexico. The instrument was successfully recovered and was flown again on September 26, 1975 at 0600 MST. Electrical conductivity, ion mobility and charge number density measurements were obtained on both flights. The data from these two experiments, as well as electrical conductivity measurements from two previously conducted subsonic blunt probe experiments, were used to study the middle atmospheric ionization variability which occurs during the early morning period.

With respect to the data, evidence has been presented to suggest that positive ion conductivity during sunrise conditions at midlatitudes is a solar dependent parameter in the altitude region above 30 km. Appreciable conductivity variations with respect to solar zenith angle were observed in the region where ionization by solar ultraviolet radiation is not considered to be significant. Subsonic Gerdien condenser and blunt probe experiments measured as much as an order of magnitude increase in ion conductivity at certain altitudes (45 km to 50 km) over a change in solar zenith angle from 90° to 53°. Ion mobility data from the Gerdien condenser experiments indicated that the increase in ion conductivity primarily resulted from an increase in ion mobility, thus suggesting the presence of a photodissociation

process for positive ions during the early morning period which results in smaller, more mobile ions.

6.2 Recommendations

More than one distinct positive ion mobility group were observed in some of the Gerdien condenser data for September 26, 1975. The instrument's ability to measure the smaller mobility species is to a significant extent dependent upon the size of the collection voltage, and thus a larger range of sweep voltages should be considered for future Gerdien condenser experiments.

The data handling and reduction capabilities could be greatly improved by the implementation of computer analysis techniques. The telemetered data format is the same for both the Gerdien condenser and the blunt probe and thus, with a greater usage anticipated for both of these instruments, the development of such computer software would be very beneficial.

Finally, the implications of using mobility data to interpret ion mass and size are beyond the scope of this thesis, but merit further consideration. A better understanding of the dependence of ion mobility on these parameters would be potentially helpful in further studying the ionization processes in the middle atmosphere.

REFERENCES

Arnold, F., D. Krankowsky and K. H. Marien, First mass spectrometric measurements of positive ions in the stratosphere, Nature 267, 30-32 (1977).

Chesworth, E. T. and L. C. Hale, Ice particulates in the mesophere, Geophys. Res. Lett. 1, 347-350 (1974).

Cipriano, J. P., L. C. Hale and J. D. Mitchell, Relations among low ionosphere parameters and A3 radio wave absorption, J. Geophys. Res. 79, 2260-2265 (1974).

Conley, T.D., Mesospheric positive ion concentration mobility and loss rates obtained from rocket-borne Gerdien condenser measurements, Radio Sci. 9, 575-592 (1974).

Croskey, C., In situ measurements of the mesosphere and stratosphere, Scientific Report No. 442, Ionosphere Research Laboratory, The Pennsylvania State University (1976).

Cuffin, N., A circular slot antenna for use on ionospheric probes, Scientific Report No. 249, Ionosphere Research Laboratory, The Pennsylvania State University (1965).

ECOM Report No. 5144, U.S. Army Electronics Command, Atmospheric Sciences Laboratory, White Sands Missile Range, New Mexico (1967).

Farrokh, H., Design of a simple Gerdien condenser for ionospheric D-region charged particle density and mobility measurements, Scientific Report No. 433, Ionosphere Research Laboratory, The Pennsylvania State University (1975).

Gerdien, H., Demonstration eines apparates zur absoluten messung der electreschen leitfahigut der luft, Terr. Magn. Atmos. Elec. 10, 65-79 (1905).

Hale, L. C. and D. P. Hoult, A subsonic D-region probe-theory and instrumentation, Scientific Report No. 247, Ionosphere Research Laboratory, The Pennsylvania State University (1965).

Israel, H. and L. Schulz, The mobility spectrum of atmospheric ions-principles of measurements and results, Terr. Magn. Atmos. Elec. 38, 285-300 (1933).

Kraakevik, J., The airborne measurement of atmospheric conductivity, J. Geophys. Res. 63, 161-169 (1958).

Mitchell, J. D., An experimental investigation of mesospheric ionization, Scientific Report No. 416, Ionosphere Research Laboratory, The Pennsylvania State University (1973).

Mitchell, J. D. and L. C. Hale, Observations of the lowest ionosphere, Space Research XIII, 471-475 (1973).

Mitchell, J. D., R. S. Sagar and R. O. Olsen, Positive ions in the middle atmosphere during sunrise conditions, Space Research XVII, 199-204 (1977).

Paltridge, G. W., Experimental measurement of the small-ion density and electrical conductivity of the stratosphere, J. Geophys. Res. 70, 2751-2761 (1965).

Pedersen, A., Measurement of ion concentration in the D-region of the ionosphere with a Gerdien condenser rocket probe, FOA 3 Report A607, Research Institute of National Defence, Stockholm, Sweden (1964).

Pontano, B. A., Rocket measurements of Nitric oxide in the lower D-region of the ionosphere, Scientific Report No. 347, Ionosphere Research Laboratory, The Pennsylvania State University (1970).

Rose, G. and H. U. Widdel, Results of concentration and mobility measurements for positively and negatively charged particle taken between 85 and 22 km in sounding rocket experiments, Radio Sci. 7, 81-87 (1972).

Stergis, C. G., S. C. Coroniti, A. Nazarek, D. E. Kotas, D. W. Seymour and J. V. Werme, Conductivity measurement in the stratosphere, J. Atmos. Terr. Phys. 6, 233-242 (1955).

Velinov, P., On ionization in the ionospheric D-region by galactic cosmic rays, J. Atmos. Terr. Phys. 30, 1891-1905 (1968).

Widdel, H. U., private communication (1975).

Widdel, H. U., G. Rose and R. Borchers, The variation of electric conductivity and ion mobility in the mesosphere between high and low solar activity measured with a rocket borne parachute Gerdien aspiration analyzer probe experiment, Report No. MPAE-W-47-76-09, Max-Planck-Institut Fur Aeromonie (1976).

Woessner, R. H., W. E. Cobb and R. H. Gunn, Simultaneous measurement of the positive and negative light-ion conductivities to 26 kilometers, J. Geophys. Res. 63, 171-180 (1958).

Zimmerman, L. E., Integrated circuit electrometer and sweep circuitry for an atmospheric probe, Scientific Report No. 376 (E), Ionosphere Research Laboratory, The Pennsylvania State University (1971).

Bourdeau, R. E., E. C. Whipple, Jr. and J. F. Clark, Analytic and experimental electrical conductivity between the stratosphere and ionosphere, J. Geophys. Res. 64, 1363-1370 (1959).

☆ U.S. GOVERNMENT PRINTING OFFICE: 1978 777-093/17